The Climatic Origins of Risk-Taking: Evidence from China

Yun Cong* Pei Gao† Yan Luo‡ Yiqing Lü§

May 2026

Abstract

Does climate history still shape modern risk-taking? Using paleoclimatic reconstructions, we build city-level measures of climate variability in China from 1500 to 1950 and link them to contemporary risk-taking across three domains: retail investors, households, and executives of listed firms. Individuals from more variable regions behave more cautiously when uncertainty rises: investors reduce trading and tilt toward safer stocks; households cut leverage and avoid entrepreneurship; CEOs reduce R&D and M&A. The effect is driven by the stochastic rather than persistent component of variability, so it is the unpredictability of adverse shocks that drives caution. In a migrant sample, the effect operates through birth-region rather than current-residence climate. We also rule out lifetime experience: contemporary (1950–2000) climate variability has no effect. Lastly, the pattern also appears in pre-modern risk-taking: high-variability regions were less likely to adopt risky cash crops in the 1930s, indicating the trait is transmitted across generations.

JEL Classification Numbers: N50, Q54, G11, D81, D91

Keywords: historical climate variability, risk taking, retail investors, households, CEOs

*Fudan University, ycong23@m.fudan.edu.cn
†National University of Singapore, p.gao@nus.edu.sg
‡Fudan University, luoyan@fudan.edu.cn
§NYU Shanghai, yiqing.lu@nyu.edu

I Introduction

There is a growing body of literature documenting that various cultural traits, including attitudes toward cooperation, trust, and gender roles, have evolved through continuous interaction between humans and the historical conditions they face (Alesina et al., 2013; Nunn and Wantchekon, 2011; Guiso et al., 2016). Among these cultural dimensions, risk preference is fundamental, shaping a broad range of economic and life decisions such as investment, savings, and innovation. Yet, compared to other cultural traits, the historical origins of risk preference remain significantly under-explored. To what extent does ancestral exposure to conditions centuries ago continue to influence modern risk-taking behavior? To address this question, we study the long-run impact of ancestral climate variability on contemporary risk-taking across diverse financial and economic domains. Our analysis provides novel evidence on the determinants of individual risk preferences and on how culture forms over history.

For most of human history, climate was the dominant source of uncertainty and adversity. Erratic weather, droughts, and floods disrupted agricultural production, threatened food security, and produced repeated, large-scale shocks long before financial or political risks existed in their modern form. This makes climate history a natural place to study the long-run origins of risk preferences. How such exposure shapes risk preferences, however, is theoretically ambiguous. Repeated negative shocks may induce risk aversion as a survival mechanism, or they may instead encourage risk-taking and innovation as a strategy to escape subsistence traps. This paper provides the first empirical evidence on these competing predictions. Prior work on the determinants of risk preferences has emphasized two channels: individual demographic characteristics such as gender and wealth (Dohmen et al., 2011; Falk et al., 2018), and direct exposure to adverse shocks such as macroeconomic crises (Malmendier and Nagel, 2011), violence (Callen et al., 2014), and natural disasters (Cassar et al., 2017). Much less is known, however, about how risk attitudes form when adversity is repeated and collective over generations. We test whether ancestral exposure to persistent, erratic weather shaped risk-averse preferences as an environmental adaptation, and whether

these traits are transmitted intergenerationally to influence decisions in modern financial and corporate settings.

China offers an ideal empirical setting to study this research question. Its size produces substantial subnational variation in historical climate risk, and a within-country design holds constant country-level confounders such as formal institutions (e.g., the centralized political system) and broader cultural factors (e.g., Confucianism). This setup allows cleaner identification of the link between historical climate variability and modern risk preferences than the cross-country frameworks common in the literature.

We link centuries of climate data to the birth regions of contemporary individuals and their observable risk-taking behaviors in multiple domains (e.g., retail investors' trading in stock markets, households' financial decisions, and top executives' corporate risk strategies). We use paleoclimatic reconstructions[1] from the Monsoon Asia Drought Atlas (Cook et al., 2010) to build prefecture-level measures of historical climate risk from 1500 to 1950. Drawing on over 300 tree-ring sites across Monsoon Asia, MADA reconstructs the summer (June–August) Palmer Drought Severity Index (PDSI), a gridded indicator of relative drought and flood severity.[2] Our primary measure of long-term climate variability is the standard deviation of PDSI, capturing the magnitude of year-over-year fluctuations; we also use the number of extreme-weather events, defined as years with $|\text{PDSI}| > 2$. To go beyond the frequency-of-extremes measures common in the literature (e.g., Kahn, 2005; Noy, 2009; Barrot and Sauvagnat, 2016), we decompose climate variability into a persistent and a stochastic component, providing a fuller picture of long-run environmental risk.

To document risk-taking behavior, we use data from three distinct economic domains. First, using a proprietary dataset from a major Chinese brokerage, we capture retail in-

[1] Paleoclimatic reconstructions are reliable scientific methods to estimate past climate conditions (e.g., temperature, precipitation, drought severity) over timescales before instrumental records. They rely on high-quality proxy data (e.g., tree ring and ice cores)—natural archives that preserve robust climate signals. These reconstructions and their data are widely used in academic literature to quantify long-term climate conditions.

[2] The focus on summer months aligns with Asia's monsoon season and covers the growing periods for China's staple crops such as rice and wheat, making climate variability directly relevant to agricultural production, food stability, and thus the formation of risk preferences.

vestors' risk-taking in the stock market through their trading activities, portfolio composition, and risk preference assessments. The demographic information enables us to identify each investor's birth city and city of residence, allowing us to isolate the effects of historical climate variability in their hometowns from those of their current residences. Second, we use the China Family Panel Studies (CFPS), a nationally representative biennial survey spanning 2014–2024, to capture household-level financial risk-taking, including households' entrepreneurial activities, leverage, and cash holdings. Finally, we analyze top corporate executives' risk-taking using data on listed firms from the China Stock Market & Accounting Research Database (CSMAR) between 2011 and 2024. Here, risk-taking is proxied by corporate R&D investment, M&A activity, and idiosyncratic volatility of stock returns.

We hypothesize that individuals' latent risk preferences are most revealed through their behavioral responses to uncertainty shocks. To test this, we employ a differences-in-differences style framework to examine whether the behavioral responses of retail investors, households, and corporate executives to contemporary uncertainty shocks vary according to the historical climate variability of their birth regions. To capture the time-varying uncertainty, we employ the VIX index and the US-China trade war as exogenous shocks for our retail investor analysis, while utilizing the China Economic Policy Uncertainty (EPU) index to capture macroeconomic and policy-related uncertainty for our household and corporate settings.

Our primary analysis leverages granular, high-frequency data on retail investors, which provides a unique laboratory for observing revealed risk preferences. The identification is a two-way fixed effect model in which we control for both individual and time fixed effects. We also include a comprehensive set of characteristics at both birth-city and the individual levels. The results show that when stock market uncertainty rises, investors from regions with greater historical climate variability reduce their stock market exposure and trading intensity, and tilt their trading towards less risky stocks, including stocks with low idiosyncratic or systematic risks and of eponymous state-owned-enterprises. Furthermore, utilizing the US-China trade war as an exogenous uncertainty shock within a difference-in-

differences framework, we document that investors from historically high-variability regions exhibit a disproportionately stronger contraction in risk-taking. Finally, our findings are robust to alternative measurements, various inference strategies, and subsample tests. We run horse-races against birth-region geographic and economic characteristics interacted with VIX, a placebo test using contemporary (1950–2000) climate variability, and a subsample of investors born in prefectures from which historical migration was prohibitively costly. In particular, our results also hold in a migrant subsample of individuals residing outside their birth regions, ruling out any confounders associated with their region of residence.

Because stock market investors are a selected group of individuals who have already chosen to participate in a risky financial market, we extend our analysis to household and corporate settings. Consistent with our baseline result using individual-level data, households from historically variable regions respond to heightened economic uncertainty by deleveraging, increasing liquidity buffers, and curtailing entrepreneurial entry. Similarly, we also document that firms led by executives from these high-variability regions adopt significantly more conservative policies during periods of macro-uncertainty, evidenced by reduced R&D expenditure, fewer mergers and acquisitions, and lower idiosyncratic stock return volatility.

After documenting the robust relationship between ancestral climate variability and modern risk aversion across multiple economic domains, we conduct tests to investigate the underlying mechanisms. First, historical climate variability is a multidimensional construct, encompassing the average magnitude of fluctuations, the frequency of extreme shocks, and the degree of stochastic unpredictability. To disentangle these dimensions, we decompose historical climate data into its persistent and stochastic components, and find that the stochastic component is the dominant driver of modern risk aversion. Our results remain robust when controlling for the cumulative frequency of extreme weather events, suggesting that the unpredictability of environmental threats, rather than their mere incidence or scale, is the fundamental force shaping persistent risk preferences.

Second, we rule out two alternative explanations for this pattern. The first is institutional:

high-variability regions may have developed distinctive local institutions, such as communal insurance arrangements, that shape risk-taking on their own. The effect, however, operates through birth-region rather than current-residence climate even among migrants, and it attenuates in port cities where contact with outsiders diluted local norms. Both findings point to a transmitted cultural trait rather than a feature of place. In addition, an influential literature links rice cultivation to cooperative, interdependent norms, raising the possibility that a rice-farming legacy underlies our results. Historical climate variability is nonetheless uncorrelated with crop suitability, and a direct horse-race interacting rice suitability with VIX rules out rice cultivation is the primary mechanism.

Lastly, we show the same risk-averse pattern predates modern financial markets, using cash crop adoption (e.g., cotton) as a proxy for historical risk-taking. In pre-industrial societies, switching from staple crops like rice or wheat to cash crops exposed households to heightened risks. We find that regions with higher historical climate variability were less likely to grow cotton, even after controlling for soil suitability. These patterns in historical agriculture align with our modern findings, suggesting that climate-shaped risk preferences have persisted and been transmitted across generations.

Our paper contributes to several strands of literature. First, we provide the first empirical evidence regarding the impact of long-term repeated exposure to adversity on risk preferences, where the direction of influence is theoretically ambiguous. Persistent instability could act as a double-edged sword: it may breed caution to ensure survival or encourage risk-taking and innovation to escape hardship. Our findings shed light on this debate by demonstrating that the dominant mechanism in this setting is caution for survival. More importantly, we show that it is not merely the frequency of negative shocks that fosters risk aversion; the nature of the risk is critical. Persistent and regular negative shocks may allow for adaptation; in contrast, unpredictable stochastic negative shocks heighten loss salience.

Second, this paper contributes to the literature on the historical origins of cultural norms. While prior research establishes that attitudes such as cooperation, trust, and gender norms

have deep historical roots (Alesina et al., 2013; Nunn and Wantchekon, 2011; Guiso et al., 2016), our study focuses on a fundamental yet understudied dimension: risk preferences. We show that climate history, a primary source of risk for most of human history, persistently shapes modern risk attitudes and decision-making.

In addition, our findings contribute to the literature on the determinants of risk preferences by bridging the gap between individual experience and cultural evolution. Prior research emphasizes the role of demographics (e.g. gender) (Dohmen et al., 2011; Falk et al., 2018), and individuals' direct personal exposure to negative shocks can shape risk attitudes (Malmendier and Nagel, 2011; Callen et al., 2014; Knüpfer et al., 2017). In contrast, we extend the temporal scope of the "experience-based learning" literature by demonstrating that ancestral collective exposure to long-term climate risks can foster a permanent shift in the distribution of risk preferences. This provides evidence that risk culture is not merely a reflection of lifetime experience, but a persistent adaptation to the environment.

Finally, we add to the literature on climate and the economy. A large body of research has documented how contemporary climatic variables affect economic and societal outcomes such as agricultural productivity, energy use, labor supply, conflict, migration, and aggregate growth (Dell et al., 2012, 2014; Buggle and Durante, 2021; Stroebel and Wurgler, 2021; Oh et al., 2026; Iyigun et al., 2024; Li et al., 2024). Different from these studies, we focus on the long-run consequences of climatic history. By showing that historical climate variability—not only the magnitude of shocks but especially their unpredictable stochastic component—is critical for shaping risk preferences and risk-taking behavior in modern settings, we uncover a novel channel through which climate risks could affect economic decisions.

We believe this paper also carries important policy implications. We highlight that climatic environment imposes not only immediate economic costs but also potential long-run cultural consequences. Persistent climatic stress may shape the risk preferences of future generations, influencing investment behavior, financial market dynamics, and asset pricing over very long horizons. Recognizing these intergenerational cultural channels is therefore

essential for designing socially optimal climate and economic policies.

Our paper is organized as follows. In Section 2, we discuss our hypotheses. In Section 3, we describe the data and variables. In Section 4, we present the main empirical results using stock market investor data. In Section 5, we extend the analysis to households and firms. In Section 6, we discuss mechanisms. Section 7 concludes.

II Hypotheses

Why might climate conditions in history potentially determine people's risk preferences and risk-taking behavior? For pre-industrial economies, climate variability was the most pervasive source of risk to livelihoods, manifesting as fluctuations in temperature, precipitation, and extreme weather events. Even in modern economies, year-to-year variations in precipitation and temperature significantly impact crop yield fluctuations (Hultgren et al., 2025; Lesk et al., 2016; Mendelsohn, 2007). In pre-industrial eras, however, this sensitivity was amplified. Without modern mitigation technologies, erratic weather rendered traditional farming ineffective. Because incomes relied almost entirely on subsistence agriculture, climate variability could translate directly into famine. Thus, regions with high climate variability faced repeated shocks that threatened not only income stability, but survival itself.

This raises a fundamental question: do threats to survival foster caution or boldness? The theoretical answer is ambiguous. On one hand, unstable environments may favor risk aversion as a survival strategy, with repeated shocks heightening loss sensitivity. Through cultural transmission, these protective traits are passed down intergenerationally (Bisin and Verdier, 2001; Doepke and Zilibotti, 2008) and continuously reinforced by centuries of exposure to adverse shocks. On the other hand, variability can spur risk-taking. Harsh conditions may encourage a "gamble for resurrection," driving innovation and experimentation to escape hardship (Rabin and Thaler, 2001; Shah et al., 2012). Empirically, households facing shocks often pivot to high-stakes activities (Bulte et al., 2018), diversify crops (Ashraf

and Michalopoulos, 2015), or strengthen communal insurance networks that enable bolder decision-making (Fafchamps, 1992; Townsend, 1994).

Climate variability has two components: a persistent component reflecting forecastable trends, and a stochastic component reflecting unpredictable shocks. This distinction lets us sharpen the prediction. Persistent shocks could allow households to adapt, through technologies, crop diversification, and communal insurance. Stochastic shocks do not; they heighten loss salience and reinforce precautionary motives. We therefore predict not simply that climate variability fosters risk aversion, but that the stochastic component matters more.

In summary, historical climate variability may foster risk aversion as a survival adaptation, or it may instead spur risk tolerance and innovation. Within the risk-aversion view, we predict that unpredictability, more than predictability, is the primary driver. This paper provides the first empirical evidence on both hypotheses and on the conditions under which these preferences form.

III Data and Variables

We link a multi-centennial climatic record with granular individual-level data based on birthplace. Section 3.1 describes how we measure long-run climate variability, Section 3.2 explains how we capture modern risk-taking using three different data sources, and Section 3.3 introduces other key variables.

3.1 Climate Variability

Climate variability constituted the primary source of economic adversity and systemic risk in pre-industrial societies. To identify regions subject to systematically higher climatic risks, we leverage historical data from the Monsoon Asia Drought Atlas (MADA) to construct measures of long-term climate instability (Cook et al., 2010).[3]

[3]Alternative sources such as instrumental weather station records (e.g., NOAA's Global Historical Climatology Network) offer finer spatial resolution, but they are unsuitable for our setting for two reasons: their

3.1.1 Data Source

Climate data comes from paleoclimatic reconstructions, which use multiple proxies such as tree rings. MADA offers a high-resolution reconstruction of Asian climate spanning 1500–2005, with grid cells measuring 2.5° latitude by 2.5° longitude (approximately 278 kilometers at the equator). These reconstructions draw from over 300 tree-ring sites across Monsoon Asia and provide estimates of the summer (June–August) Palmer Drought Severity Index (PDSI), a gridded measure of relative moisture computed from both temperature and precipitation, ranging from −10 (extreme drought) to +10 (extreme wetness).

We employ MADA as our primary paleoclimate source for two reasons: First, MADA offers exceptionally long temporal coverage, with the reconstruction extending as far back as 1300. Because fewer tree-ring sites contribute before 1500, our main analysis uses the denser post-1500 window, with the longer 1300–1950 record as a robustness check. Second, its focus on summer months aligns with the growing periods for China's staple crops, rice and wheat, making our measure of weather variability directly relevant to agricultural production and food stability in China.[4] Appendix Figure A.6 documents the reliability of the MADA reconstruction: Panel (a) shows that MADA tracks the independent NOAA 20th Century Reanalysis over their 1842–1950 overlap window, and Panel (b) maps the geographic distribution of reconstruction quality across prefectures.

3.1.2 Historical Climate Variability Measures

We measure historical climate variability at the prefecture level, since this is the resolution at which we identify investors' hometowns. For each measure below, we construct two versions:

coverage begins only in the 19th century at the earliest, and station density expanded substantially over time, so the accuracy of regional climate measures from station records varies systematically across periods. MADA's tree-ring proxy network provides the consistent multi-centennial coverage that station-based records cannot.

[4]For China, cotton, rice, and wheat are among the most widespread and economically significant crops. Using data from the Food and Agriculture Organization's Global Agro-Ecological Zones (GAEZ) project (FAO and IIASA, 2021), as shown in Appendix Figure A.1, we identify February–September as the primary growing season for wetland rice and wheat.

one over the historical period 1500–1950, which captures the climate conditions faced by an individual's ancestors, and one over the contemporary period 1950–2000, which serves as a placebo. Since all individuals in our modern data were born after 1950, this separation lets us isolate the long-run cultural channel from any direct lifetime-experience effect.

Our primary measure is the standard deviation of the PDSI. We compute the standard deviation of PDSI for each grid cell over 1500–1950, σ_i, then average using zonal statistics across all cells within a prefecture to yield a regional measure of variability.[5] We adopt this as our baseline metric because it captures the magnitude of variability and is widely used in the literature. Panel A of Figure 1 and Figure A.2 map this measure across Chinese prefectures, revealing substantial spatial heterogeneity. Notably, the spatial pattern does not align with China's economic development pattern (the wealthy southeast versus the interior). As a robustness measure, we also use the frequency of weather disasters, defined as the number of years with $|\text{PDSI}| > 2$.[6] This proxy captures the most severe magnitudes of climate variability and is widely used for extreme climate events. The two measures are highly correlated, further validating our measurement approach.

Beyond magnitude, climate variability has a temporal dimension: a region experiencing frequent but regular shocks differs fundamentally from one facing unpredictable events. We therefore decompose historical climate variability into a persistent and a stochastic component using an autoregressive model of order 5 (AR(5)). The persistent component is the standard deviation of the fitted values, capturing low-frequency trends and long-run structural shifts. The stochastic component is the standard deviation of the residuals, capturing unpredictable short-term shocks that leave little room for adaptation.

Finally, to verify that our historical climate variability measure is not associated with confounders that might also affect risk-taking, Appendix Table B.1 shows that it is uncorrelated

[5] Appendix A illustrates examples of how MADA grids are mapped into a single prefecture.

[6] PDSI is centered at zero, with negative values representing dry conditions and positive values wet (e.g., PDSI < -2 indicates moderate drought; PDSI < -4 indicates extreme drought). The $|\text{PDSI}| > 2$ threshold is widely used in climatology to distinguish moderate-to-extreme moisture anomalies from near-normal conditions.

with indicators of current economic development (e.g., 2024 night light intensity), proxies for historical agricultural intensity (e.g., soil suitability for staple crops), and measures of regional governance quality (e.g., provincial capital status). As expected, some geographic features (e.g., proximity to the coastline, latitude, and elevation) are correlated with climate variability; we address this by including individual fixed effects in our preferred specification, which absorb all time-invariant birth-city characteristics.

3.2 Measuring Risk-Taking in Modern Settings

To measure risk-taking in modern settings, we use data on three domains: stock market trading behavior, household financial choices, and CEOs' corporate risk strategies. Summary statistics are reported in Table 1 for the retail investor sample, and in Appendix Tables C.1 and C.2 for the household and corporate samples.

3.2.1 Individual Stock Market Trading

We measure individual investors' stock market trading behavior using a proprietary dataset from a major Chinese brokerage firm. It contains account-level information on risk preferences, trading behaviors (e.g., transactions and asset holdings), and demographic characteristics (including birthplace and residential place) over January 2017 to December 2022. Table 1 reports summary statistics.

Sample Construction. We apply several filters. First, we restrict the sample to individuals born between 1951 and 2000. The upper bound reflects A-share participation rules, which require investors to be at least 18; the lower bound keeps all sample births after our historical climate window (1500–1950), so that personal lifetime experience does not overlap with the historical exposure we measure. Second, to focus on investors with meaningful financial stakes, we exclude those with a portfolio size below 10,000 RMB (approximately 1,389 USD). Third, we exclude inactive investors, defined as those with fewer than 10 trades over the full sample period (following Liao et al., 2022). Finally, we exclude accounts showing

signs of irregular activity, such as algorithmic trading labels. From the remaining eligible investors, we randomly select 500,000 individuals using city-capped sampling, retaining up to 50,000 investors per birth city. This prevents large cities such as Shanghai and Shenzhen from dominating the sample, which would over-weight low-variability regions and bias our estimates. We then aggregate trading data to the investor-quarter panel. The resulting sample spans 294 of 368 modern Chinese prefectures, with near-complete coverage within China proper; Appendix Figure A.8 maps the geographic distribution of the sample.

Measuring Risk Tolerance. The brokerage provides a static risk preference score obtained from a mandatory questionnaire at account opening. Scores range from one to five, with higher values indicating greater risk tolerance. Although the static nature of this measure prevents us from capturing dynamic shifts in preferences, it offers a useful snapshot of an investor's risk attitudes. We use this elicited measure as motivating evidence in Section 4.1.

Measuring Risk-Taking Behavior. We capture individuals' risk-taking behavior from two dimensions: their trading intensity and their portfolio choices toward risky stocks. First, trading intensity captures an investor's active exposure to the stock market. When uncertainty rises, risk-averse investors reduce exposure by trading less frequently and shifting from net buying toward net selling. We construct three measures of market exposure and trading intensity in both transaction value and count: $BuyMore_{it}$, a dummy that equals one if the number of buy trades exceeds that of sell trades, and zero otherwise; $NetTrade_{i,t}$, the difference between the number of purchases and sales; and $NetRatio_{i,t}$, which is $NetTrade_{i,t}$ scaled by the sum of purchase and sale counts. We prioritize count-based over value-based measures in our main tests because they are less sensitive to portfolio size and passive price movements, and more directly capture how actively an investor acts on directional conviction. As a robustness check, we also use value-based trading measures.

Measuring Risky-Stock Selection. We capture investors' tendency to tilt their trading toward risky stocks. We use three measures of stock-level risk. The first is idiosyncratic volatility, computed from the market model by regressing daily returns on market returns

over the one-year period ending in quarter $t-1$ (requiring at least 60 days of return data). The second is the stock's market beta (its sensitivity to market returns), from the same regression. The third, following Pursiainen (2022), is an indicator for non-eponymous stocks: we identify eponymous stocks as state-owned firms whose names include words such as "China" or "Sino"; retail investors perceive these stocks as less risky because the names evoke implicit government backing. We construct all three risk-tilt measures using the normalized metric:

$$100 \times \frac{\sum_k (NetBuy_{i,k,t} \times RiskMeasure_{k,t})}{\sum_k |NetBuy_{i,k,t}|}, \tag{1}$$

where $NetBuy_{i,k,t}$ is investor i's net trades on stock k in quarter t (buys minus sells), and $RiskMeasure_{k,t}$ is one of the three stock-level risk measures defined above. Substituting in turn the three measures yields $IvolTilt_{i,t}$, $BetaTilt_{i,t}$, and $NonEpTilt_{i,t}$.

3.2.2 Households' Decisions

To extend our analysis to a more representative population, we examine households' risk-taking using survey data from the China Family Panel Studies (CFPS), a nationally representative biennial longitudinal survey administered by Peking University's Institute of Social Science Survey (ISSS). CFPS collects data at the individual, family, and community levels on topics including economic activities, migration status, and household financial decisions.

Sample Construction. We use data from the 2014–2022 waves, as only surveys from 2014 onward include information on migration status and housing loans. Consistent with the brokerage data filters, we restrict CFPS observations to respondents born after 1950.

Measuring Financial Risk-Taking Behavior. We measure household financial risk-taking through three behaviors: entrepreneurial activity, financial leverage, and cash holdings. Entrepreneurship is widely recognized as a key indicator of risk-taking, as launching a business entails substantial uncertainty and potential loss (e.g., Moskowitz and Vissing-Jørgensen, 2002; Hurst and Pugsley, 2011). A higher leverage ratio signals risk tolerance

through amplified exposure to financial gains and losses (Domowitz and Sartain, 1999), and a lower cash ratio reflects reduced liquidity preference and greater willingness to invest in risky assets (Guiso et al., 1996). We construct three variables: (1) $Entrepreneur_{i,t}$, a dummy equal to one if any household member operates a private business and zero otherwise; (2) $FinLev_{i,t}$, the ratio of total debt (excluding housing mortgages) to total assets; and (3) $CashRatio_{i,t}$, the ratio of cash holdings to total assets. We exclude housing mortgages from the debt ratio because they represent long-term, secured borrowing for essential needs rather than speculative financial risk.

3.2.3 Executives' Corporate Risk Strategies

We also examine top executives' corporate decision-making using data on Chinese A-share listed firms (2011–2024) from CSMAR. Unlike the trading and CFPS data, where hometowns are observed at city level, CEOs' birthplaces are not mandatorily disclosed in CSMAR; for most CEOs we observe only the province of birth. We therefore examine whether historical climate variability in the CEO's birth province influences corporate decisions.

Sample Construction. Corporate strategies face governance constraints that personal trading and household decisions do not. To ensure firm strategies reflect the top executive's risk preferences, we restrict the sample to private firms in which the CEO also serves as board chairman—the setting in which managerial discretion is highest.

Measuring Corporate Risk-Taking Behavior. We construct three variables: (i) R&D expenditures scaled by lagged total assets, capturing innovation risk; (ii) the number of M&As initiated in year t, capturing deal risk; and (iii) idiosyncratic stock return volatility computed from daily returns relative to the market model, capturing operational risk.

3.3 Other Variables

3.3.1 Uncertainty Shocks

Latent risk preferences are most clearly revealed through behavioral responses to uncertainty shocks, so we construct measures of time-varying uncertainty for our analyses. In the retail investor analysis, we use the VIX index for the SZ50, a measure of expected volatility in the Chinese stock market. We also exploit the onset of the US-China trade war as an exogenous uncertainty shock, defining a binary indicator equal to one from 2018 Q3 onward, when tariffs were formally imposed.

For the household and firm analyses, where responses extend beyond stock-market turbulence, we use China's Economic Policy Uncertainty (EPU) index. The index, constructed following Baker et al. (2016), measures uncertainty from the frequency of uncertainty-related keywords in newspaper coverage.[7]

3.3.2 Control Variables

Economic Control. To control time-varying economic development at the birth-city level, we include annual GDP per capita and GDP growth rate.

Individual Time-varying Controls. We also include investor-specific stock market exposure from the prior quarter, i.e., account return, total trading value, total number of trades, number of traded stocks, and maximum portfolio value. We include the squared term of the investor's age to account for any nonlinear life-cycle effect on investment.

Geographic Controls. To ensure the effect of historical climate variability is not confounded by other geographic factors, we control for a set of birth-city geographic variables and allow their effects to vary over time: terrain ruggedness, a coastal-region dummy, logarithm of land area, latitude, and longitude (FAO–GAEZ database).

[7]The data is available from `https://www.policyuncertainty.com/index.html`.

IV Climate Variability in History and Modern Risk-Taking: Evidence from the Stock Market

4.1 Motivational Evidence: Elicited Risk Preference

Before examining how investors react to specific uncertainty shocks, we first establish the baseline relationship between historical climate variability and individual risk preferences. This serves as a vital validity check for our underlying mechanism: long-term erratic weather patterns cultivate risk-averse preferences.

We proxy for risk attitudes using the mandatory risk-preference assessment completed by individual investors upon opening stock market accounts. This elicited measure offers a standardized, self-reported, and time-invariant snapshot of an investor's psychological predisposition toward risk. Panel B of Figure 1 displays the cross-regional variation in risk preferences across Chinese cities, with darker colors indicating higher risk tolerance. Appendix Figure A.7 further shows that the distribution of risk tolerance score shifts systematically between regions with below-median and above-median historical climate variability. Table 2 formally presents the cross-sectional regression results. Across all specifications, the coefficient on historical climate variability is negative and statistically significant. These results provide critical empirical support for the preference channel, confirming that exposure to long-term environmental volatility produces deep-seated risk aversion.

4.2 Empirical Strategy

In this section, we examine whether historical climate variability in individuals' birth cities influences their risk-taking behavior in the stock market, a high-stakes domain characterized by significant financial exposure, particularly under conditions of substantial market uncertainty. To capture dynamic risk preferences, we construct revealed risk measures based on actual trading activity. Unlike the static elicited risk preference measure, these metrics al-

low us to observe how risk-taking adjusts in response to evolving market environments. Our baseline identification uses a two-way fixed effect model in which we control for individual and time fixed effects. We also include a comprehensive set of time-varying characteristics at both the individual and birth-city levels. Our baseline specification is:

$$Y_{i,c,j,t} = \alpha + \beta \, \textit{Hist. Climate Var}_c \times VIX_{t-1} + \lambda X_{c,t} + \mu Z_{i,t} + r_i + W_t + \varepsilon_{i,q}, \qquad (2)$$

where $Y_{i,c,j,t}$ represents the trading behavior of individual i from birth city c, currently residing in city j, during quarter t. We measure risk-taking ($Y_{i,c,j,t}$) along two dimensions using six alternative metrics: *trading activities*, which capture general exposure to the stock market, and *risk tilts*, which capture the tendency to trade riskier stocks. The variable of interest is the interaction between historical climate variability and market uncertainty. We measure the historical climate variability of an individual's birth city (*Hist. Climate Var*) using the standard deviation of the PDSI between 1500 and 1950. To capture forward-looking market volatility, we use the lagged implied volatility derived from SZ50 index options. Specifically, we construct VIX_{t-1} by taking the quarterly average of daily implied volatility and subtracting 10. The coefficient β on this interaction term is our key estimate; it identifies how latent risk preferences, shaped by climate history, manifest in trading behavior during periods of heightened uncertainty.

In our preferred specification, we include individual fixed effects (r_i), which absorb all time-invariant individual characteristics (e.g., age, gender, education, and birth-city geographical characteristics). We also include quarter fixed effects (W_t) to capture common temporal shocks that affect all investors. To control for time-varying local economic conditions, we include birth-city GDP per capita and GDP growth rate ($X_{c,t}$). Furthermore, to account for dynamic investor behavior, we control for a vector of lagged stock market exposure variables ($Z_{i,t-1}$): account return, total trading value, number of trades, number of stocks held, and maximum portfolio value. Finally, we include the squared term of the

investor's age to capture nonlinear life-cycle effects. Standard errors are clustered at the birth-city level, consistent with the level of treatment variation.

Identification Challenges. Our identification rests on three features: (i) climate variability over 1500–1950 is pre-determined relative to the lifetime of any individual in our sample; (ii) our preferred specification includes individual fixed effects that absorb all time-invariant individual and birth-city characteristics; and (iii) the interaction with VIX shocks provides identification similar to a difference-in-differences design, where high- and low-climate-variability investors are compared before and after uncertainty rises.

However, some potential concerns nonetheless still remain. First, other birth-region characteristics correlated with historical climate variability (e.g., geography) may also influence risk-taking. Second, an investor's ancestors may not have always lived in the birth city; if historical migration was systematically correlated with climate, this could bias our estimates. Third, contemporaneous climate exposure during investors' lifetimes may also shape preferences. Fourth, the differential VIX response we attribute to climate variability may instead reflect other cross-regional differences, such as financial sophistication or local industry composition. For any of these concerns to bias our estimates, the underlying factor must both correlate with historical climate variability and differentially shape investors' responses to VIX. We will further provide corresponding robustness checks to address each of these concerns in Section 4.3.

4.2.1 Main Results: Trading Intensity

Table 3 examines how historical climate variability affects trading intensity during periods of market fluctuation. We use three outcome variables to capture trading intensity. Columns (1)–(3) examine *BuyMore*, a dummy that equals one if the number of buy trades exceeds the number of sell trades. Columns (4)–(6) examine *NetTrade*, defined as the difference between the number of buy and sell trades. Columns (7)–(9) examine *NetRatio*, calculated as *NetTrade* divided by the number of trades. We prioritize trade count-based measures

over value-based measures to mitigate potential biases arising from portfolio size and price movements; results using trade value-based measures are reported in Appendix Table B.3.

For each outcome, we report three specifications of increasing saturation. The first is the most basic, including only quarter and province fixed effects together with birth-city-level controls, which allows cross-sectional variation across cities. The second replaces province fixed effects with individual fixed effects, which absorb all time-invariant birth-city characteristics. Columns (3), (6), and (9) report our preferred specification, adding lagged individual-level trading controls to the second specification.

Across all columns, the coefficient estimates for the interaction term between historical climate variability and VIX are negative and statistically significant. This indicates that when facing higher market uncertainty (i.e., a higher VIX), investors from regions with high historical climate variability reduce their net buying activity, behavior consistent with heightened risk aversion. One thing worth noting is that the estimates remain stable in magnitude when switching from the basic specification to the preferred specification. As the preferred specification further includes individual fixed effects that absorb all time-invariant individual and birth-city characteristics (e.g., wealth, education, gender, and geographic features of the birth region), this stability indicates that the effect is not driven by these confounders.

The economic magnitude of these results is meaningful. For instance, in Column (9), where *NetRatio* is the outcome, the interaction coefficient implies that for the same uncertainty shock, high-exposure investors exhibit a negative shift in their *NetRatio* of 0.12 points. Relative to the sample mean (5.06), this corresponds to a **2.4%** relative decline in net buying intensity. Although the effect is small relative to the high overall volatility of individual trading ratios (SD = 35.06), long-term variable climate systematically shifts the mean of net buying pressure during market stress.

In Appendix Table B.3, we demonstrate robustness by replacing the trade count measures with value-based counterparts; the findings remain consistent. Overall, our baseline results

indicate that during uncertainty shocks, individuals from regions with greater historical climate variability exhibit a stronger propensity to reduce risk exposure, revealing a distinct risk-averse preference.

4.2.2 Risk Tilt

In Table 4, we report results for three risk-tilt measures, each representing the trade-weighted directional 'tilt' of an investor's portfolio toward specific risk characteristics. As defined in Section 3.2.1: *Idiosyncratic Risk Tilt* (Columns 1–3), capturing tilt toward stocks with high idiosyncratic volatility; *Systematic Risk Tilt* (Columns 4–6), capturing tilt toward stocks with high market exposure; and *Speculative Tilt* (Columns 7–9), capturing tilt toward non-eponymous stocks.

Across all columns, the coefficient estimates for the interaction term between historical climate variability and VIX are significantly negative. This indicates that during periods of aggregate market volatility, investors with higher exposure to historical climate risk actively shift their portfolios away from high-risk, high-beta, and non-guaranteed assets, exhibiting a stronger preference for safety relative to the average investor. In Appendix Table B.3, we replace the count-based risk-tilt measures with their value-based counterparts; the findings remain consistent.

Taken together, this section demonstrates: whether measured by trading intensity or their tilt toward risky stocks, investors from regions with high historical climate variability significantly reduce their risk exposure during periods of market uncertainty.

4.3 Robustness Checks

4.3.1 Placebo Test: Historical vs. Contemporary Climate Variability

The primary difficulty in identifying the effect of long-term climate variability on risk preferences is that contemporaneous climate exposure may also directly shape preferences. To circumvent this problem, we focus on climate variability over 1500–1950, which is pre-

determined relative to the lifetime of any individual in our sample. We conduct a horse-race test, reported in Table 5, that includes a measure of contemporary climate variability (1950–2000) alongside our primary historical measure (1500–1950).

Even after controlling for climate patterns within investors' lifetimes (all our investors were born after 1950), the coefficient on the interaction between historical climate variability and VIX remains statistically significant and economically large. In contrast, the contemporary variability measure is either insignificant or, in some specifications, has an opposing sign. This provides strong evidence that the observed differences in risk-taking behavior in the stock market are shaped by deep-rooted historical experiences, rather than by the more recent weather patterns experienced during an individual's lifetime.

4.3.2 Birth-City Confounders

A primary empirical concern is that some other birth-region characteristic, rather than historical climate variability, drives the observed differences in modern risk-taking. For such a confounder to fully explain our results, it would have to satisfy three demanding conditions simultaneously: (i) be correlated with our 1500–1950 PDSI variability measure, (ii) interact with stock-market uncertainty to predict trading behavior, and (iii) operate through the investor's birth region rather than their current residence.

We first show that the most likely candidates do not even satisfy condition (i). Appendix Table B.1 reports that our climate-variability measure is uncorrelated with a broad set of birth-region characteristics, including proxies for historical agricultural intensity (soil suitability for staple crops) and current economic development (2024 night-light intensity, provincial-capital status, distance to the Yangtze River). The only characteristics that are correlated with climate variability are geographic features—coastal status, latitude, and elevation—which is mechanically expected, since climate is partly determined by geography.

We therefore subject geographic features—the one class of birth-region characteristics that does satisfy condition (i)—to a direct horse-race test in Panel A of Table 6, which

interacts a battery of birth-region geographic characteristics (latitude, longitude, elevation, coastal status, land area, and distance to the Yangtze River) with VIX alongside our main interaction term. If the baseline result reflected birth-region geography rather than climate variability, the coefficient on *Hist. Climate Var* $\times$ VIX would attenuate or lose significance. Instead, the coefficient remains negative and statistically significant across all six outcomes, with magnitudes comparable to the baseline estimates in Tables 3 and 4. Appendix Table B.5 further confirms this under a stricter specification, in which each geographic feature is allowed its own time-varying effect by being interacted with quarter fixed effects; the climate-variability coefficient again remains negative and significant.

Panel B of Table 6 provides a complementary check using birth-region economic characteristics. We directly horse-race their VIX interactions against *Hist. Climate Var* $\times$ VIX as a more stringent test. The coefficient on *Hist. Climate Var* $\times$ VIX again remains negative and significant across all six outcomes; the GDP and rice-suitability interactions are themselves significant in places but do not displace the climate-variability effect.

Together, these tests show that the climate-variability effect is not displaced either by the geographic profile of the birth region (Panel A) or by its economic and agricultural profile (Panel B). While we cannot rule out every possible omitted variable, any such factor would still need to satisfy the three demanding conditions above, a combination difficult to reconcile with any single rival explanation.

4.3.3 Ruling Out Historical Migration Bias

One natural concern is that an investor's ancestors may not have always lived in their birth city, raising the possibility that historical migration could bias our estimates. First, even if historical migration occurred, it would bias our estimates only if migration patterns were systematically correlated with climate variability. Random migration with respect to climate would only lead to attenuation bias, working against finding a significant result.[8]

[8]Historical migration across city and provincial boundaries was rare in pre-industrial China, so the bulk of the modern population in a given prefecture is descended from ancestors who experienced the same long-run

The only plausible threat is selective migration, meaning that risk-tolerant individuals systematically left high-variability regions. This would mechanically widen the modern gap between high- and low-variability prefectures. To rule this out, we construct an *escape cost* variable measuring the terrain-adjusted migration cost from each prefecture to its nearest prefecture in a lower climate-variability quartile.[9] Where escape cost is high, historical migration to a more stable climate was difficult, so selection through migration could not have operated. We restrict our sample to investors born in prefectures with the highest escape cost. Appendix Table B.7 (Panel A) shows that the effect remains significant in this subsample and comparable in magnitude to the full-sample estimate, indicating that climate-motivated historical migration does not drive our findings.

4.3.4 Other Robustness Checks

We conduct several additional robustness checks to further validate our baseline findings. The results remain robust when using an alternative measure of historical climate variability based on the frequency of extreme shocks (Appendix Table B.2) and when using alternative outcome variables for stock-market risk-taking (Appendix Table B.3). We also show our finding holds when restricting the sample to prefectures for which the underlying paleoclimate reconstruction is of higher quality (Appendix Table B.6).[10]

climate conditions.

[9]The escape-cost measure is the terrain-adjusted travel time from a prefecture to the nearest prefecture one quartile lower in historical climate variability (quartiles based on the standard deviation of summer PDSI, 1500–1950). Construction details are provided in Appendix Section A5, and Appendix Figure A.9 illustrates the underlying cost surface, the per-prefecture escape cost, and the high-escape-cost subsample used in Appendix Table B.7, Panel A.

[10]The precision of a prefecture's climate series depends on how many independent reconstruction cells fall within its boundaries. We treat a prefecture as having "high-quality" MADA data when its polygon contains at least two valid MADA grid-cell centers, so that the aggregated series reflects genuine spatial averaging rather than a single cell's reconstruction (about two-thirds of prefectures, 232 of 368; results are similar under the stricter requirement of at least three cells, which holds for about one-third of prefectures).

4.4 The US-China Trade War as an Exogenous Shock

While our baseline analysis uses VIX to capture uncertainty, VIX is itself endogenous to market conditions and investor expectations. To address potential endogeneity concerns and validate our results, we exploit the escalation of the US-China trade war in Q3 2018 as a distinct, exogenous uncertainty shock to China's stock market. We use a difference-in-differences framework, replacing VIX in the baseline interaction term with *TradeWar*, an indicator equal to one for quarters from Q3 2018 onward and zero before. The interaction of interest becomes *Hist. Climate Var* $\times$ *TradeWar*.

Table 7 reports the DID results. Across all specifications, the coefficient on the interaction term remains significantly negative, indicating that investors from regions with high historical climate variability curtailed their risk exposure following the onset of the trade war. Figure 2 presents the event-study graph. The key assumption of our DID approach is that, without the trade war, trading intensity of investors from high-variability regions would have followed parallel trends with those from low-variability regions. Figure 2 shows that the gap between high- and low-variability investors is flat across all outcome variables over the three quarters preceding the trade war, supporting the parallel trends assumption. Following the shock in Q3 2018, which was marked by heightened market panic, investors from regions with high historical climate variability exhibit an immediate and substantial decline in trading intensity and a shift toward low-risk stocks, with the gap persisting for at least three quarters.

V Beyond the Stock Market: Evidence from Households and Firms

Section 4 establishes that retail investors from regions with higher historical climate variability are less likely to adopt risky trading strategies, particularly when market uncertainty rises. Because stock market investors represent a selected group of individuals, we extend the analysis to two broader populations: ordinary households (Section 5.1), which include both

equity-market participants and non-participants, and top executives of listed Chinese firms (Section 5.2). This allows us to test whether the climate–risk-taking relationship generalizes beyond the brokerage sample.

5.1 Household Risk-Taking (CFPS)

We employ an alternative data source—the China Family Panel Studies (CFPS), a biennial household survey—which provides detailed data on birthplace, residential location, demographic information, and various household financial decisions. We draw on information about households' decisions on asset allocation and financial leverage to measure their risk-taking. Our sample includes the 2014–2022 waves,[11] as variables on migration status and household housing loans are only available from 2014 onward. Consistent with the brokerage data filters, we restrict CFPS observations to respondents born after 1950. Since households respond to economic fluctuations beyond just stock market signals, we replace the VIX index with China's Economic Policy Uncertainty (EPU) index to capture broader economic sentiment.[12] We calculate yearly EPU as the average of the monthly EPU, scaled by 100. Historical climate variability is measured at the city level of the husband's hometown (i.e., the survey's main interviewee), as we only have information on the hometown of the main interviewees. Appendix Table C.1 shows the summary statistics.

First, we construct three variables to capture household-level risk-taking financial behaviors: (1) whether a household member is an entrepreneur; (2) the ratio of total debt to total assets (excluding housing mortgages); and (3) the ratio of cash holdings to total assets. The results are reported in Table 8. In Columns (1), (3), and (5), we report the main results using the interaction between the prior quarter's EPU and historical climate variabil-

[11]The baseline survey started in 2010, with follow-up surveys conducted every two years. The CFPS sample spans 25 provinces/municipalities/autonomous regions, targeting 16,000 households and all family members within them. Pilot surveys with initial and follow-up visits occurred in 2008–2009 across Beijing, Shanghai, and Guangdong, with official fieldwork launching in 2010. Baseline family members from the 2010 survey, plus their future biological or adopted children, are designated as permanent "gene members" for tracking.

[12]The index is constructed following the methodology of Baker et al. (2016), using data from mainland Chinese newspapers.

ity (1500–1950). This examines whether economic and political uncertainty elicits stronger risk aversion among individuals from hometowns with more variable climate histories. In Columns (2), (4), and (6), we conduct horse-race tests by including both the historical interaction and an additional interaction between the EPU index and contemporary climate variability (1950–2000), to check whether the effects are driven by preferences shaped by climate variability in history or by climate experiences during individuals' lifetimes.

The results provide robust evidence supporting our hypothesis and align with the baseline findings. In Columns (1), (3), and (5), the interaction coefficients between historical climate variability and EPU are significant across all risk-taking measures: propensity to start an enterprise, financial leverage, and cash-holding ratio. These indicate that households reduce risk exposure when facing heightened uncertainty. In Columns (2), (4), and (6), the historical interaction effects hold after including the competing contemporary interaction, except in Column (4), where the coefficient for financial leverage remains negative but becomes insignificant. The contemporary interaction shows no significant effects across all three columns, suggesting that risk preferences shaping household financial decisions are molded not by lifetime climate experiences, but by historical climate patterns that foster enduring cultural norms passed down across generations. Appendix Table C.3 further shows that the same pattern obtains when we replace the standard deviation of PDSI with the frequency of extreme weather shocks, confirming that the household result is not driven by the particular climate-variability measure used.

5.2 Corporate Risk-Taking (CSMAR)

As a further check on external validity, we examine whether historical climate variability also shapes corporate risk-taking in CSMAR's sample of Chinese A-share listed firms. CSMAR reports CEOs' birthplaces only at the province level, so we link historical climate variability to corporate decisions at the province level rather than the prefecture level used in earlier sections. Despite this coarser geographic resolution, the firm analysis offers a useful

test of whether the pattern documented for individuals and households extends to corporate decision-making, where key strategic choices are largely made by executives whose risk attitudes were shaped during their formative years.

We capture three distinct dimensions of corporate risk-taking and link them to the CEO's birth-province climate variability. Our outcome variables are: R&D expenditures scaled by total assets, merger and acquisition (M&A) activity, and idiosyncratic stock return volatility. The sample is restricted to non-state-owned firms whose CEO also serves as board chairman, where managerial discretion is highest. Summary statistics are reported in Appendix Table C.2. Table 9 presents the results. As in Table 8, Columns (1), (3), and (5) report results including only the interaction between EPU and historical climate variability, while Columns (2), (4), and (6) further test the role of contemporary climate. We control for time-varying macroeconomic conditions and firm financial characteristics, as well as firm, year, and birth-province fixed effects. Standard errors are clustered at the birth-province and firm levels. The results show that firms led by CEOs from regions with greater historical climate instability respond more strongly to economic uncertainty: they cut R&D spending, conduct fewer M&As, and exhibit lower stock return volatility. The contemporary climate's influence is either insignificant or shows the opposite sign, confirming that the risk preferences driving these corporate behavior changes do not stem from current weather conditions.

In short, this section uses two additional data sources, the China Family Panel Studies and CSMAR, to extend our stock-market findings to households and firms. Combined with our stock market evidence in Section 4, the results span three independent domains and three independent samples. Across all three, individuals from regions with greater historical climate variability exhibit persistent risk-averse preferences that manifest in risk-averse decisions during uncertainty shocks.

VI Exploring the Mechanisms

The evidence presented so far reveals a robust relationship between historical climate variability and individuals' risk-taking in modern settings. This finding supports the hypothesis that unstable environments gave rise to risk-averse preferences as a survival strategy. In this section, we conduct several tests to explore the mechanisms through which this impact persists over centuries.

6.1 Mechanism: Stochastic vs. Persistent Climate Variability

The first and most important mechanism we examine is which dimension of climate risk shapes modern risk-taking. Beyond magnitude, climate variability has a temporal dimension. A region experiencing frequent but regular extreme shocks differs fundamentally from one facing unpredictable events. This distinction is critical for identifying the precise channel through which historical climate variability shapes risk preferences. Persistent weather shocks may allow households to adapt over time, while stochastic shocks heighten loss salience and reinforce precautionary motives. Our prediction is therefore that the stochastic component drives the effect more than the persistent component.

We decompose historical climate variability into persistent and stochastic components using an autoregressive model of order 5 (AR(5)). The persistent component is the standard deviation of the fitted values, reflecting predictable long-run structural shifts. The stochastic component is the standard deviation of the residuals, capturing unpredictable short-term shocks. Appendix Figure A.5 maps the two components across Chinese prefectures, showing that the persistent and stochastic dimensions of climate variability capture distinct sources of historical risk. In Table 10, we replicate our baseline tests from Tables 3 and 4 but replace the standard deviation of PDSI with its two components, Persistent Variability and Stochastic Variability. We also control for the frequency of climate disasters (*DisasterFreq*) and its interaction with VIX_{t-1}, to test explicitly whether our variance measures capture

information beyond the simple incidence of historical climate disasters.

The coefficient on the stochastic component is consistently negative and statistically significant. In contrast, the effect of persistent variability is smaller in magnitude and less robust; in some specifications it even becomes positive. This pattern confirms our sharper prediction: stochastic variability, not persistent variability, is the primary driver of risk-averse behavior during uncertainty shocks. The frequency of extreme shocks consistently yields negative estimates, indicating that more frequent shocks also contribute to regional risk aversion. However, conditional on the number of shocks, the unpredictability of these events is what primarily drives the impact.

In short, our results uncover an underlying mechanism through which climate experience shapes risk preferences. The frequency of negative weather shocks contributes to risk aversion, but the unpredictability of those shocks is the more important driver: regular shocks leave room for adaptation, while unpredictable stochastic shocks heighten loss salience and reinforce precautionary motives. This finding distinguishes our analysis from a generic "climate variability matters" claim.

6.2 Ruling Out Alternative Channels

Our central hypothesis is that long-run climate variability fostered a persistent culture of caution toward risk. A direct implication is that the effect should be weaker wherever that culture was diluted. If risk attitudes are transmitted as local norms, regions with greater historical contact with outsiders, whose traditional norms were eroded by cultural mixing, should show a smaller effect. We test this using coastal-city status as a proxy for historical openness. China's coastal prefectures hosted the major treaty ports and maritime-trade hubs that channelled centuries of contact with foreign populations and ideas, so their local norms are systematically less insulated than those of interior prefectures.[13] Appendix Table

[13]The 19th-century treaty ports (e.g., Shanghai, Guangzhou, Tianjin, Ningbo, Fuzhou, Xiamen) were almost exclusively coastal, and even earlier maritime trade flowed through coastal entrepôts, so a coastal indicator captures the bulk of historical exposure to outsiders without requiring us to take a stand on which

B.7, Panel B shows that the climate-variability effect is no longer significant in the coastal subsample, consistent with cultural transmission: where historical exposure to outsiders eroded local norms, the climate-shaped risk preference fades.

This cultural-transmission account competes with two natural alternatives. The first is institutional: regions with more variable climate histories may have developed distinctive local institutions, such as stronger communal insurance arrangements or weaker formal property rights, that shape modern risk-taking on their own. The second is agronomic: an influential literature links rice cultivation to interdependent and cooperative norms, so the pattern we document could instead reflect a rice-farming legacy. We address each in turn and find that neither displaces the climate-variability effect.

The Institutional Channel. We test the institutional channel using a migrant subsample of investors whose current city of residence differs from their birth city (approximately 20% of the sample). If the effect operated through local institutions rather than transmitted preferences, it should track an investor's current residence rather than their birth region. The specification includes the historical climate variability of both the birth city and the current city, each interacted with VIX. Table 11 reports the results. The birth-city interaction is negative and statistically significant across all six outcomes, while the current-residence interaction is weaker and less robust. Risk-taking thus tracks where an investor was raised, not where they now live, which rules out local institutions as the main driver.

Rice Cultivation Channel. A second alternative draws on the rice theory of culture, which holds that paddy-rice agriculture, with its demands for coordinated irrigation and reciprocal labor exchange, fostered interdependent and cooperative norms distinct from those of wheat-farming regions (Talhelm et al., 2014). Because paddy rice also buffers households against idiosyncratic shocks through communal labor-sharing, a rice-farming heritage could plausibly produce the caution we attribute to climate variability. But a rice legacy can confound our estimates only if it is correlated with historical climate variability, and Appendix Table B.1

specific year a port was "opened."

shows that our 1500–1950 PDSI variability measure is uncorrelated with birth-region soil suitability for staple crops. We also subject rice suitability to the same horse-race we applied to geographic and economic confounders. Panel B of Table 6 interacts birth-region rice suitability with VIX alongside our main interaction term. The rice-suitability interaction is significant in some columns, consistent with the rice theory carrying independent explanatory power, but it does not displace *Hist. Climate Var* $\times$ VIX, which remains negative and significant across all six outcomes. The climate-variability effect therefore survives a direct test against the rice-farming legacy.

6.3 Historical Persistence: Cash Crop Adoption in the 1930s

If climate-shaped risk aversion is a deep cultural trait, the same pattern should be visible in pre-modern risk-taking decisions, not just in modern financial markets. We test this prediction using cash crop adoption in 1930s China.

In pre-industrial agrarian societies, the choice between staple crops (rice, wheat) and cash crops (cotton) was itself a risk-taking decision. Staple crops offered reliable subsistence and predictable yields. Cash crops exposed farmers to market fluctuations, price volatility, and the loss of an edible fallback. If prices collapsed or harvests failed for cotton, farmers risked famine without self-sufficiency buffers. We therefore use whether a county cultivated cotton in the 1930s as a proxy for historical agricultural risk-taking. We also use a sharper proxy: among cotton-growing counties, whether they adopted the newly-introduced American cotton variety. American cotton was introduced to China in the early twentieth century, and adopting it carried additional uncertainty over yield, local adaptation, and market acceptance. Switching to a novel, untested variety was the riskier choice; native cotton was the safer option for a farmer already committed to cotton.

We collect data on cotton cultivation from a county-level census conducted by the Chinese Cotton Industry Statistics Association in the early 1930s. The census reports each county's planted area for both American and native cotton varieties. Since we lack time

variation, we estimate the relationship cross-sectionally, regressing cotton adoption choices on historical climate variability over 1500–1900, ending before the cotton data to ensure predetermination. Table 12 reports the results. Columns (1), (2), (4), and (5) show that regions with higher historical climate variability were less likely to cultivate cotton, controlling for soil suitability for cotton relative to staple crops. Columns (3) and (6) restrict the sample to cotton-growing counties and show that historical climate variability is negatively associated with the adoption of the (riskier) American variety. Both patterns confirm that the climate-shaped risk-taking signal we document in modern financial settings was already operating in pre-modern agricultural decisions, predating modern stock markets by centuries.

In short, the same risk-averse pattern that drives modern financial behavior also predicts who took crop-choice risks in the 1930s. This historical persistence is exactly what a cultural-transmission account predicts: if risk preferences are shaped by long-run climate exposure and passed down across generations, they should appear consistently across historical periods and across domains where risk is at stake.

VII Conclusion

This paper asks how long-term climate variability shapes modern risk-taking. Using paleoclimatic reconstructions from MADA, we measure historical climate variability across Chinese prefectures from 1500 to 1950 and link it to risk-taking in three modern domains: retail investors' trading, households' financial decisions in the China Family Panel Studies, and corporate executives' strategies in listed firms. Across all three, individuals from regions with greater historical climate variability behave more cautiously under uncertainty. Retail investors reduce trading and tilt toward safer assets; households cut leverage, avoid entrepreneurship, and hold more cash; firms led by CEOs from high-variability regions reduce R&D, M&A activity, and stock return volatility. The pattern survives a difference-in-differences design around the US-China trade war, a placebo using contemporary (1950–

2000) climate variability, horse-races against geographic and economic confounders, and a migration-cost subsample.

We also explore a series of mechanism tests. First, decomposing climate variability into persistent and stochastic components reveals that the stochastic, unpredictable component is the primary driver: it is the unpredictability of climate shocks, more than their frequency, that produces risk-averse preferences. Second, the effect operates through birth-region rather than current-residence climate even for migrants who have relocated, ruling out local institutions as the operative channel. Third, the effect attenuates where historical exposure to outsiders diluted local cultural norms, as a cultural-transmission mechanism would predict. Fourth, the same risk-averse pattern is visible in 1930s agricultural decisions, where regions with higher historical climate variability were less likely to cultivate cotton and less likely to adopt the riskier American cotton variety, predating modern financial markets by decades. Together, these findings indicate that ancestral exposure to repeated and unpredictable climatic instability gave rise to risk-averse cultural norms, transmitted intergenerationally through families and communities, and that these norms remain salient in modern economic contexts where climate no longer directly affects most financial decisions.

Our results add risk preferences to the list of cultural traits shaped by historical experience, and identify climate history as a novel source of persistent differences across individuals and societies. They also carry policy implications: climate change affects not only contemporary economic outcomes but also the cultural and behavioral traits of future generations, a long-run channel relevant for the design of climate and economic policy.

References

Alesina, Alberto, Paola Giuliano, and Nathan Nunn. 2013. "On the Origins of Gender Roles: Women and the Plough." *Quarterly Journal of Economics*, 128(2): 469–530, DOI: http://dx.doi.org/10.1093/qje/qjt005.

Ashraf, Quamrul, and Stelios Michalopoulos. 2015. "Climatic Fluctuations and the Diffusion of Agriculture." *Review of Economics and Statistics*, 97(3): 589–609, DOI: http://dx.doi.org/10.1162/REST_a_00486.

Baker, Scott R., Nicholas Bloom, and Steven J. Davis. 2016. "Measuring Economic Policy Uncertainty." *Quarterly Journal of Economics*, 131(4): 1593–1636, DOI: http://dx.doi.org/10.1093/qje/qjw024.

Barrot, Jean-Noël, and Julien Sauvagnat. 2016. "Input Specificity and the Propagation of Idiosyncratic Shocks in Production Networks." *Quarterly Journal of Economics*, 131(3): 1543–1592, DOI: http://dx.doi.org/10.1093/qje/qjw018.

Bisin, Alberto, and Thierry Verdier. 2001. "The Economics of Cultural Transmission and the Dynamics of Preferences." *Journal of Economic Theory*, 97(2): 298–319, DOI: http://dx.doi.org/10.1006/jeth.2000.2678.

Buggle, Johannes C., and Ruben Durante. 2021. "Climate Risk, Cooperation and the Co-Evolution of Culture and Institutions." *Economic Journal*, 131(637): 1947–1987, DOI: http://dx.doi.org/10.1093/ej/ueaa127.

Bulte, Erwin, Lihe Xu, and Xiaobo Zhang. 2018. "Post-Disaster Aid and Development of the Manufacturing Sector: Lessons from a Natural Experiment in China." *European Economic Review*, 101 441–458, DOI: http://dx.doi.org/10.1016/j.euroecorev.2017.10.014.

Callen, Michael, Mohammad Isaqzadeh, James D. Long, and Charles Sprenger. 2014. "Violence and Risk Preference: Experimental Evidence from Afghanistan." *American Economic Review*, 104(1): 123–148, DOI: http://dx.doi.org/10.1257/aer.104.1.123.

Cassar, Alessandra, Andrew Healy, and Carl von Kessler. 2017. "Trust, Risk, and Time Preferences After a Natural Disaster: Experimental Evidence from Thailand." *World Development*, 94 90–105, DOI: http://dx.doi.org/10.1016/j.worlddev.2016.12.042.

Cook, Edward R., Kevin J. Anchukaitis, Brendan M. Buckley, Rosanne D. D'Arrigo, Gordon C. Jacoby, and William E. Wright. 2010. "Asian Monsoon Failure and Megadrought During the Last Millennium." *Science*, 328(5977): 486–489, DOI: http://dx.doi.org/10.1126/science.1185188.

Dell, Melissa, Benjamin F. Jones, and Benjamin A. Olken. 2012. "Temperature Shocks and Economic Growth: Evidence from the Last Half Century." *American Economic Journal: Macroeconomics*, 4(3): 66–95, DOI: http://dx.doi.org/10.1257/mac.4.3.66.

Dell, Melissa, Benjamin F. Jones, and Benjamin A. Olken. 2014. "What Do We Learn from the Weather? The New Climate-Economy Literature." *Journal of Economic Literature*, 52(3): 740–798, DOI: http://dx.doi.org/10.1257/jel.52.3.740.

Doepke, Matthias, and Fabrizio Zilibotti. 2008. "Occupational Choice and the Spirit of Capitalism." *Quarterly Journal of Economics*, 123(2): 747–793, DOI: http://dx.doi.org/10.1162/qjec.2008.123.2.747.

Dohmen, Thomas, Armin Falk, David Huffman, Uwe Sunde, Jürgen Schupp, and Gert G. Wagner. 2011. "Individual Risk Attitudes: Measurement, Determinants, and Behavioral Consequences." *Journal of the European Economic Association*, 9(3): 522–550, DOI: http://dx.doi.org/10.1111/j.1542-4774.2011.01015.x.

Domowitz, Ian, and Robert L. Sartain. 1999. "Determinants of the Consumer Bankruptcy Decision." *Journal of Finance*, 54(1): 403–420, DOI: http://dx.doi.org/10.1111/0022-1082.00110.

Fafchamps, Marcel. 1992. "Solidarity Networks in Preindustrial Societies: Rational Peasants with a Moral Economy." *Economic Development and Cultural Change*, 41(1): 147–174, DOI: http://dx.doi.org/10.1086/452001.

Falk, Armin, Anke Becker, Thomas Dohmen, Benjamin Enke, David Huffman, and Uwe Sunde. 2018. "Global Evidence on Economic Preferences." *Quarterly Journal of Economics*, 133(4): 1645–1692, DOI: http://dx.doi.org/10.1093/qje/qjy013.

Guiso, Luigi, Tullio Jappelli, and Daniele Terlizzese. 1996. "Income Risk, Borrowing Constraints, and Portfolio Choice." *American Economic Review*, 86(1): 158–172.

Guiso, Luigi, Paola Sapienza, and Luigi Zingales. 2016. "Long-Term Persistence." *Journal of the European Economic Association*, 14(6): 1401–1436, DOI: http://dx.doi.org/10.1111/jeea.12177.

Hultgren, Andrew, Tamma Carleton, Michael Delgado, Diana R. Gergel, Michael Greenstone, Trevor Houser, Solomon Hsiang, Amir Jina, Robert E. Kopp, Steven B. Malevich, Kelly E. McCusker, Terin Mayer, Ishan Nath, James Rising, Ashwin Rode, and Jiacan Yuan. 2025. "Impacts of Climate Change on Global Agriculture Accounting for Adaptation." *Nature*, 642 644–652, DOI: http://dx.doi.org/10.1038/s41586-025-09085-w.

Hurst, Erik, and Benjamin Wild Pugsley. 2011. "What Do Small Businesses Do?" *Brookings Papers on Economic Activity*, 2011(2): 73–118, DOI: http://dx.doi.org/10.1353/eca.2011.0017.

Iyigun, Murat, Joris Mueller, and Nancy Qian. 2024. "The Intensifying Effects of Prolonged Climate Change on Conflict, 1400–1900 CE." *AEA Papers and Proceedings*, 114 80–83, DOI: http://dx.doi.org/10.1257/pandp.20241058.

Kahn, Matthew E. 2005. "The Death Toll from Natural Disasters: The Role of Income, Geography, and Institutions." *Review of Economics and Statistics*, 87(2): 271–284, DOI: http://dx.doi.org/10.1162/0034653053970339.

Knüpfer, Samuli, Elias Rantapuska, and Matti Sarvimäki. 2017. "Formative Experiences and Portfolio Choice: Evidence from the Finnish Great Depression." *Journal of Finance*, 72(1): 133–166, DOI: http://dx.doi.org/10.1111/jofi.12469.

Lesk, Corey, Pedram Rowhani, and Navin Ramankutty. 2016. "Influence of Extreme Weather Disasters on Global Crop Production." *Nature*, 529(7584): 84–87, DOI: http://dx.doi.org/10.1038/nature16467.

Li, Qing, Hongyu Shan, Yuehua Tang, and Vincent Yao. 2024. "Corporate Climate Risk: Measurements and Responses." *Review of Financial Studies*, 37(6): 1778–1830, DOI: http://dx.doi.org/10.1093/rfs/hhae001.

Liao, Jingchi, Cameron Peng, and Ning Zhu. 2022. "Extrapolative Bubbles and Trading Volume." *Review of Financial Studies*, 35(4): 1682–1722, DOI: http://dx.doi.org/10.1093/rfs/hhab070.

Malmendier, Ulrike, and Stefan Nagel. 2011. "Depression Babies: Do Macroeconomic Experiences Affect Risk Taking?" *Quarterly Journal of Economics*, 126(1): 373–416, DOI: http://dx.doi.org/10.1093/qje/qjq004.

Mendelsohn, Robert. 2007. "What Causes Crop Failure?" *Climatic Change*, 81(1): 61–70, DOI: http://dx.doi.org/10.1007/s10584-005-9009-y.

Moskowitz, Tobias J., and Annette Vissing-Jørgensen. 2002. "The Returns to Entrepreneurial Investment: A Private Equity Premium Puzzle?" *American Economic Review*, 92(4): 745–778, DOI: http://dx.doi.org/10.1257/00028280260344452.

Noy, Ilan. 2009. "The Macroeconomic Consequences of Disasters." *Journal of Development Economics*, 88(2): 221–231, DOI: http://dx.doi.org/10.1016/j.jdeveco.2008.02.005.

Nunn, Nathan, and Leonard Wantchekon. 2011. "The Slave Trade and the Origins of Mistrust in Africa." *American Economic Review*, 101(7): 3221–3252, DOI: http://dx.doi.org/10.1257/aer.101.7.3221.

Oh, Sangmin S., Ishita Sen, and Ana-Maria Tenekedjieva. 2026. "Pricing of Climate Risk Insurance: Regulation and Cross-Subsidies." *Journal of Finance*, DOI: http://dx.doi.org/10.1111/jofi.70029, Forthcoming.

Pursiainen, Vesa. 2022. "Cultural Biases in Equity Analysis." *Journal of Finance*, 77(1): 163–211, DOI: http://dx.doi.org/10.1111/jofi.13095.

Rabin, Matthew, and Richard H. Thaler. 2001. "Anomalies: Risk Aversion." *Journal of Economic Perspectives*, 15(1): 219–232, DOI: http://dx.doi.org/10.1257/jep.15.1.219.

Shah, Anuj K., Sendhil Mullainathan, and Eldar Shafir. 2012. "Some Consequences of Having Too Little." *Science*, 338(6107): 682–685, DOI: http://dx.doi.org/10.1126/science.1222426.

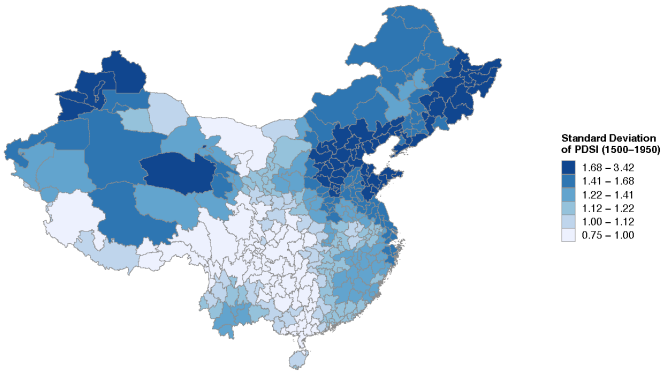
Stroebel, Johannes, and Jeffrey Wurgler. 2021. "What Do You Think About Climate Finance?" *Journal of Financial Economics*, 142(2): 487–498, DOI: http://dx.doi.org/10.1016/j.jfineco.2021.08.004.

Talhelm, Thomas, Xuemin Zhang, Shigehiro Oishi, Chen Shimin, Dongyuan Duan, Xuezhao Lan, and Shinobu Kitayama. 2014. "Large-scale psychological differences within China explained by rice versus wheat agriculture." *Science*, 344(6184): 603–608.

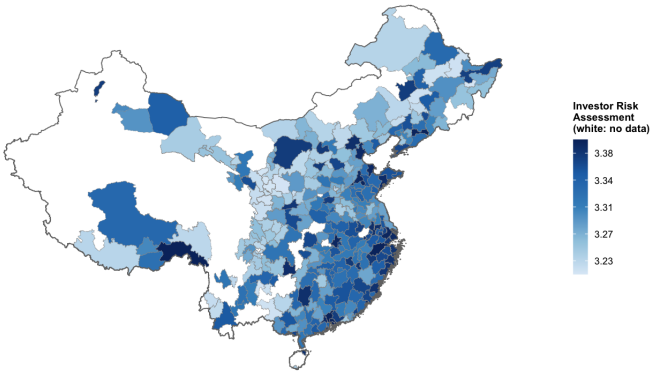
Townsend, Robert M. 1994. "Risk and Insurance in Village India." *Econometrica*, 62(3): 539–591, DOI: http://dx.doi.org/10.2307/2951659.

Figures

Figure 1: Historical Climate Variability and Risk Preference



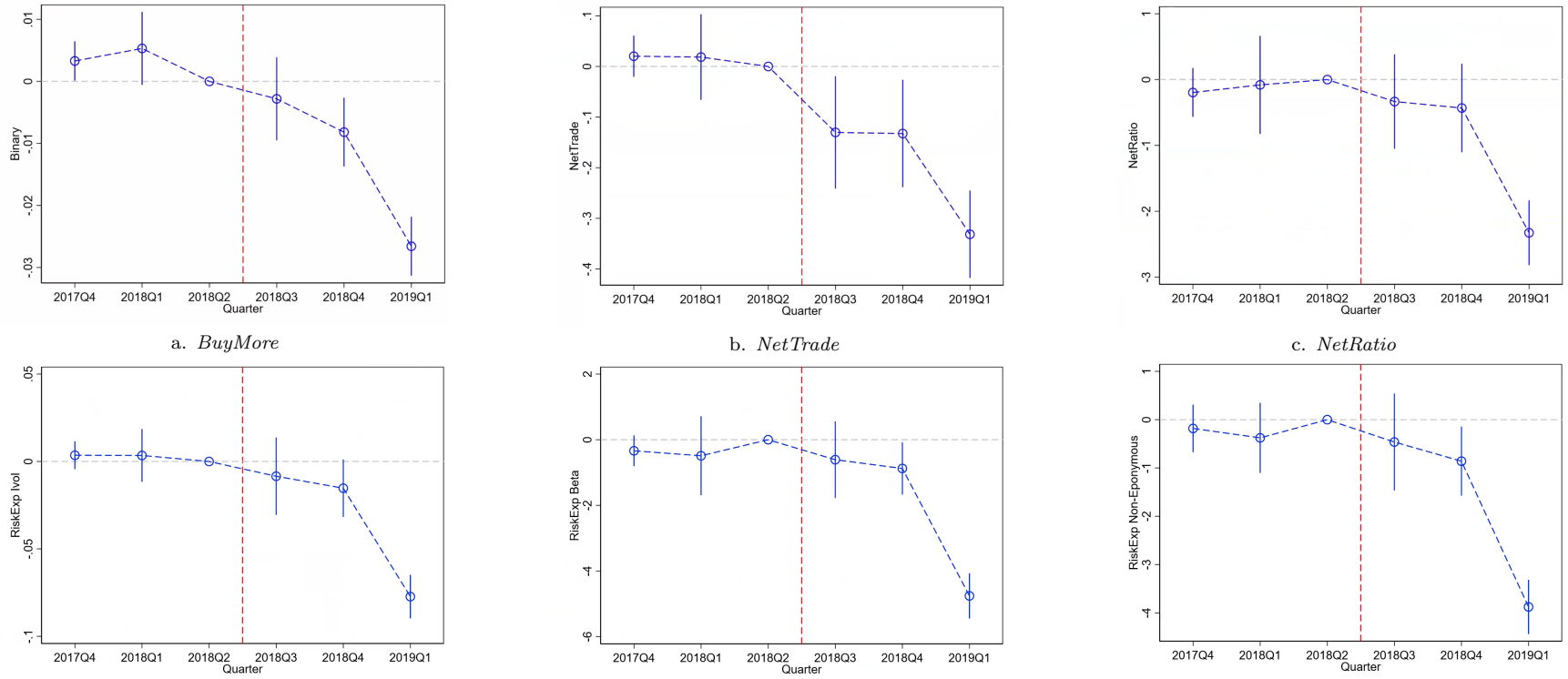
a. Historical climate varability: SD of PDSI (1500-1950)



b. City-level Individual Investor Risk Assessment

Panel A of this figure displays prefecture-level climate variability in Mainland China, measured by the standard deviation of the summer (June–August) Palmer Drought Severity Index (PDSI) from the Monsoon Asia Drought Atlas (MADA). We construct the standard deviation of PDSI between 1500 and 1950 to capture the long-term climate variability for a region. Darker shades indicate historical climatic variability. The spatial pattern of historical variability does not closely mirror current economic development, with wealthier southeastern provinces contrasting with poorer interior provinces. Panel B shows the assessed risk tolerance for individual investors in the modern setting. Darker shades indicate greater risk tolerance.

Figure 2: Event Study: The US–China Trade War as an Uncertainty Shock



a. *BuyMore* b. *NetTrade* c. *NetRatio*

d. *IvolTilt* e. *BetaTilt* f. *NonEpTilt*

This figure presents event-study estimates using the US–China trade war as an exogenous uncertainty shock to the stock market. We estimate the differential trading behavior of investors from high- versus low-historical-climate-variability regions over the 2017Q4–2019Q1 period. The vertical red dashed line marks the onset of the trade war in Q2 2018, coinciding with the U.S. announcement of Section 301 tariffs (March 23, 2018) and China's retaliatory tariff list (April 4, 2018). Panels (a)–(c) display results for three trading-intensity measures capturing exposure to market risk: $BuyMore$ is a dummy that equals one if the number of buy trades exceeds sell trades, and zero otherwise, $NetTrade$ is the difference between the number of buy and sell trades, and $NetRatio$ is $NetTrade$ divided by the number of total trades. Panels (d)–(f) capture risk-taking behavior via portfolio tilts toward risky characteristics: idiosyncratic volalitity ($IvolTilt$), beta ($BetaTilt$), and non-eponymous stocks ($NonEpTilt$), identified as state-owned firms whose names include words such as "China" or "Sino". Circles represent point estimates from the interaction of historical climate variability with quarter dummies; vertical lines indicate 90% confidence intervals. Parallel pre-trends and a sharp post-shock divergence are evident in all panels.

Tables

Table 1: Summary Statistics for Main Variables

Var.	No.	Mean	Std	P10	Median	P90
Climate Measures:						
Historical Climate Variability	7,764,502	1.3153	0.4247	0.9420	1.1865	2.0007
Contemporary Climate Variability	7,764,502	1.9120	0.4497	1.4647	1.7347	2.6764
Trading Intensity Measures:						
BuyMore	7,764,502	0.3908	0.4879	0	0	1
NetTrade	7,764,502	2.5267	7.6347	-1	0	8
NetRatio	7,764,502	5.3144	33.2005	-13.1313	0	33.3333
Risky Stock Selection (Portfolio Tilt):						
IvolTilt	7,764,502	0.4236	1.4410	-1.1956	0	2.3761
BetaTilt	7,764,502	0.2202	0.7819	-0.6278	0	1.3018
NonEpTilt	7,764,502	14.7295	50.9277	-42.8571	0	100.0000
Controls on Trading Activities:						
QtrRtn	7,764,502	-0.0182	0.1228	-0.1672	0	0.1183
TotalValue	7,764,502	577,217.2425	1476016.4659	0	42,115.0000	1546363.0000
TotalTrade	7,764,502	28.2587	58.1924	0	5	82
StockNum	7,764,502	6.1997	10.5917	0	2	17
StkHolding	7,764,502	61,664.3235	103,897.6973	0	17,223.0000	187,280.0000
Age	7,764,502	38.4664	9.8442	28	36	52

Notes: This table presents summary statistics for the key variables used in the analysis. *Historical Climate Variability* is defined as the standard deviation of a city's PDSI from 1500 to 1950, and *Contemporary Climate Variability* is the standard deviation of PDSI from 1950 to 2000. *VIX* denotes the quarterly average of the SZ50 daily VIX index minus 10. *BuyMore* equals 1 if the buy transaction count exceeds the sell. *NetTrade* is the difference between buy transaction count and sell. *NetRatio* is *NetTrade* scaled by the investor's total transaction count. *IvolTilt* (*BetaTilt*) captures the relative weight investors place on buying high idiosyncratic volatility (high beta) stocks versus low idiosyncratic volatility (low beta) stocks, in %. *NonEpTilt* measures the relative weight placed on non-eponymous stocks, in %. *TotalValue* (*TotalTrade*) is the total stock transaction value (transaction count) for an investor in a given quarter. *StockNum* is the number of unique stocks traded, and *StkHolding* is the maximum stock balance within a quarter. *Age* is the investor's exact age in a given quarter, determined by whether the investor has reached their birthday during that quarter. All continuous variables are winsorized at the 1% and 99% levels.

Table 2: Historical Climate Variability and Risk Assessment

	Risk Assessment Level		
Dep. Var.	(1)	(2)	(3)
Hist. Climate Var.(1500-1950)	-0.013*	-0.014**	-0.019**
	(0.0078)	(0.0070)	(0.0075)
Demographic Control	Y	Y	Y
Asset Control		Y	Y
Birth City-Level Controls			Y
Observations	398,086	398,086	398,086
R-squared	0.059	0.069	0.069

Notes: This table analyzes the impact of historical climate instability in an investor's hometown on their self-reported risk tolerance. The dependent variable is a risk assessment score ranging from 1 (lowest) to 5 (highest). *Hist. Climate Var.* is the standard deviation of prefecture-level PDSI from 1500–1950. All investors in our sample were born after 1950. Registered professional investors are excluded, as they are not required to undergo risk assessment. For each investor, we retain the first available quarterly observation and control for the maximum stock holding in that quarter. The model includes economic variables and geographic controls for the investor's birth city. Demographic fixed effects (gender, education, birth year-month, account open year-month, job type, and province of residence) are included. All continuous variables are winsorized at the top and bottom 1% levels. Standard errors are clustered at the investor's hometown city level and are reported in parentheses. *** $p < 0.01$, ** $p < 0.05$, * $p < 0.10$.

Table 3: Historical Climate Variability and Investor Trading Intensity

Dep. Var.	(1)	(2)	(3)	(4)	(5)	(6)	(7)	(8)	(9)
	BuyMore			*NetTrade*			*NetRatio*		
Hist. Climate Var.× *VIX*	-0.0008***	-0.0008***	-0.0007***	-0.0132***	-0.0123***	-0.0099***	-0.0199***	-0.0203***	-0.0224***
	(0.0001)	(0.0001)	(0.0001)	(0.0020)	(0.0020)	(0.0016)	(0.0072)	(0.0073)	(0.0075)
Hist. Climate Var.	-0.0004			0.0181			0.0623		
	(0.0018)			(0.0301)			(0.0917)		
Quarter FE	Y	Y	Y	Y	Y	Y	Y	Y	Y
Individual FE		Y	Y		Y	Y		Y	Y
Birth-City Controls	Y	Y	Y	Y	Y	Y	Y	Y	Y
Individual Trading Controls			Y			Y			Y
Observations	7,764,502	7,764,502	7,764,502	7,764,502	7,764,502	7,764,502	7,764,502	7,764,502	7,764,502
R-squared	0.009	0.240	0.269	0.006	0.394	0.446	0.005	0.102	0.109

Notes: This table examines whether the historical climate variability of an investor's hometown affects their risk-taking, captured by trading intensity, during periods of heightened market uncertainty. We use three variables to capture trading intensity: *BuyMore* equals one if the number of buy trades exceeds sell trades, *NetTrade* is the difference between the number of buy and sell trades, and *NetRatio* is *NetTrade* divided by total trades. *Hist. Climate Var.* is the standard deviation of prefecture-level PDSI (1500–1950). *VIX* is the quarterly average of the daily SZ50 VIX index minus 10. Birth-city control variables include city-level GDP per capita and GDP growth (both lagged by one year), and individual-level characteristics include lagged quarterly account return, the number of trades, total value of trades, the number of unique stocks traded, maximum stock balance, and age squared. All continuous variables are winsorized at the 1% and 99% levels. Standard errors are clustered at the investor's hometown city level and are reported in parentheses. *** $p < 0.01$, ** $p < 0.05$, * $p < 0.10$.

Table 4: Historical Climate Variability and Risky Stock Selection

Dep. Var.	(1)	(2)	(3)	(4)	(5)	(6)	(7)	(8)	(9)
	Idiosyncratic Risk *(IvolTilt)*			Systematic Risk *(BetaTilt)*			Speculative Tilt *(NonEpTilt)*		
Hist. Climate Var.× VIX	-0.0023***	-0.0022***	-0.0021***	-0.0009***	-0.0008***	-0.0008***	-0.0618***	-0.0582***	-0.0582***
	(0.0004)	(0.0004)	(0.0004)	(0.0002)	(0.0002)	(0.0002)	(0.0128)	(0.0130)	(0.0130)
Hist. Climate Var.	-0.0078**			-0.0035			-0.2920**		
	(0.0040)			(0.0023)			(0.1395)		
Quarter FE	Y	Y	Y	Y	Y	Y	Y	Y	Y
Individual FE		Y	Y		Y	Y		Y	Y
Birth-City Controls	Y	Y	Y	Y	Y	Y	Y	Y	Y
Individual Trading Controls			Y			Y			Y
Observations	7,764,502	7,764,502	7,764,502	7,764,502	7,764,502	7,764,502	7,764,502	7,764,502	7,764,502
R-squared	0.005	0.158	0.168	0.008	0.139	0.148	0.005	0.147	0.157

Notes: This table examines whether the historical climate variability of an investor's hometown affects their propensity to hold risky assets during periods of market uncertainty. The dependent variables represent the trade-weighted directional "tilt" of an investor's portfolio toward specific risk characteristics. Columns 1–3 examine *Idiosyncratic Risk (IvolTilt)*, based on idiosyncratic volatility. Columns 4–6 examine *Systematic Risk (BetaTilt)*, defined as the product of stock beta and market return volatility. Columns 7–9 examine *Non-Eponymous Tilt (NonEpTilt)*. We identify *eponymous stocks* as state-owned firms whose names include words such as "China" or "Sino"; thus, *NonEpTilt* captures the tendency to trade stocks lacking this implied government guarantee. The tilt measure is calculated as: $100 \times \left(\sum_k \left(NetBuy_{i,k,t} \times RiskMetric_{k,t}\right)\right) / \left(\sum_k |NetBuy_{i,k,t}|\right)$. *Hist. Climate Var.* is the standard deviation of prefecture-level PDSI (1500–1950). *VIX* is the quarterly average of the daily SZ50 VIX index minus 10. Controls and specifications generally follow Table 2. Standard errors are clustered at the investor's hometown city level and are reported in parentheses. *** $p < 0.01$, **$p < 0.05$, *$p < 0.1$.

Table 5: Placebo: Historical vs. Contemporary Climate Variability

Dep. Var.	(1)	(2)	(3)	(4)	(5)	(6)
	Trading Intensity			Risky Stock Selection		
	BuyMore	*NetTrade*	*NetRatio*	*IvolTilt*	*BetaTilt*	*NonEpTilt*
Hist. Climate Var. × *VIX*	-0.0007***	-0.0122***	-0.0403***	-0.0029***	-0.0011***	-0.0819***
	(0.0002)	(0.0025)	(0.0115)	(0.0006)	(0.0003)	(0.0197)
Cont. Climate Var. × *VIX*	0.0001	0.0027	0.0218**	0.0010**	0.0003	0.0288*
	(0.0001)	(0.0024)	(0.0109)	(0.0005)	(0.0003)	(0.0169)
Quarter FE	Y	Y	Y	Y	Y	Y
Individual FE	Y	Y	Y	Y	Y	Y
Baseline Controls	Y	Y	Y	Y	Y	Y
Observations	7,764,502	7,764,502	7,764,502	7,764,502	7,764,502	7,764,502
R-squared	0.269	0.446	0.109	0.168	0.148	0.157

Note: This table reports a placebo test for the historical-climate-variability × VIX interaction, using the same six outcomes as Tables 3 and 4. Each specification includes the interaction of VIX with historical climate variability (*Hist. Climate Var.*, the standard deviation of prefecture-level PDSI from 1500–1950) and, simultaneously, the interaction of VIX with contemporary climate variability (*Cont. Climate Var.*, the standard deviation of PDSI from 1950–2000). *VIX* is the quarterly average of the daily SZ50 VIX index minus 10. Control variables and specifications follow Table 3. All continuous variables are winsorized at the top and bottom 1% levels. Individual- and quarter-fixed effects are included. Standard errors are clustered at the investor's hometown city level and are reported in parentheses. *** $p < 0.01$, ** $p < 0.05$, * $p < 0.10$.

Table 6: Robustness: Ruling Out Confounders

Dep. Var.	(1)	(2)	(3)	(4)	(5)	(6)
	Trading Intensity			Risky Stock Selection		
	BuyMore	*NetTrade*	*NetRatio*	*IvolTilt*	*BetaTilt*	*NonEpTilt*
Panel A: Birth-Region Geographic Features						
Hist. Climate Var. × *VIX*	-0.0004**	-0.0075***	-0.0201	-0.0011**	-0.0007**	-0.0331*
	(0.0002)	(0.0027)	(0.0126)	(0.0006)	(0.0003)	(0.0200)
Latitude × *VIX*	-0.0133	-0.0896	0.0425	-0.0444	-0.0156	-1.0682
	(0.0126)	(0.1903)	(0.8652)	(0.0382)	(0.0222)	(1.4096)
Longitude × *VIX*	-0.0235	-0.2234	-0.5936	-0.0937**	-0.0168	-2.5159*
	(0.0143)	(0.2117)	(0.9214)	(0.0409)	(0.0217)	(1.4914)
Elevation × *VIX*	-0.0003	-0.0045**	-0.0270***	-0.0011**	-0.0006***	-0.0330**
	(0.0002)	(0.0021)	(0.0089)	(0.0005)	(0.0002)	(0.0151)
Coastal × *VIX*	-0.0002	-0.0043**	-0.0240**	-0.0009**	-0.0003	-0.0278*
	(0.0001)	(0.0021)	(0.0101)	(0.0004)	(0.0002)	(0.0156)
Area × *VIX*	-0.0000	-0.0001	-0.0003	-0.0000	-0.0000*	-0.0008*
	(0.0000)	(0.0001)	(0.0003)	(0.0000)	(0.0000)	(0.0005)
Dist to Yangtze River× *VIX*	0.0073	0.2260	-0.0783	-0.0349	0.0066	-0.6439
	(0.0275)	(0.3437)	(1.5351)	(0.0816)	(0.0381)	(2.5762)
Quarter FE	Y	Y	Y	Y	Y	Y
Individual FE	Y	Y	Y	Y	Y	Y
Baseline Controls	Y	Y	Y	Y	Y	Y
Observations	7,764,502	7,764,502	7,764,502	7,764,502	7,764,502	7,764,502
Panel B: Birth-Region Economic Features						
Hist. Climate Var. × *VIX*	-0.0004***	-0.0046***	-0.0005	-0.0013***	-0.0004*	-0.0275**
	(0.0001)	(0.0016)	(0.0076)	(0.0004)	(0.0002)	(0.0134)
Rice Suitability × *VIX*	0.0000**	0.0000***	0.0000***	0.0000***	0.0000***	0.0000***
	(0.0000)	(0.0000)	(0.0000)	(0.0000)	(0.0000)	(0.0000)
GDP per capita × *VIX*	-0.0051***	-0.1228***	-0.5028***	-0.0195***	-0.0071***	-0.6765***
	(0.0013)	(0.0171)	(0.0935)	(0.0040)	(0.0023)	(0.1471)
Quarter FE	Y	Y	Y	Y	Y	Y
Individual FE	Y	Y	Y	Y	Y	Y
Baseline Controls	Y	Y	Y	Y	Y	Y
Observations	7,764,502	7,764,502	7,764,502	7,764,502	7,764,502	7,764,502

Note: This table reports two horse-race robustness checks for the historical climate variability × VIX interaction, using the same six outcomes as Tables 3 and 4. Panel A adds, alongside the main interaction of VIX with historical climate variability, the interaction of VIX with a battery of birth-region geographic characteristics: latitude, longitude, elevation, coastal status, land area, and distance to the Yangtze River. Panel B adds the interaction of VIX with two birth-region economic characteristics: city-level GDP per capita and rice soil suitability. Across both panels, the coefficient on *Hist. Climate Var.* × VIX remains negative and statistically significant, indicating that the effect is not displaced by these geographic or economic characteristics of the birth region. Control variables and specifications follow Table 3. Standard errors are clustered at the investor's hometown city level and are reported in parentheses. *** $p < 0.01$, ** $p < 0.05$, * $p < 0.10$.

Table 7: Event Study: US–China Trade War Shock

Dep. Var.	(1)	(2)	(3)	(4)	(5)	(6)
	Trading Intensity			Risky Stock Selection		
	BuyMore	*NetTrade*	*NetRatio*	*IvolTilt*	*BetaTilt*	*NonEpTilt*
Hist. Climate Var. × *TradeWar*	-0.0117***	-0.1603***	-0.6337***	-0.0304***	-0.0215***	-1.2393***
	(0.0026)	(0.0301)	(0.1947)	(0.0074)	(0.0037)	(0.2845)
Quarter FE	Y	Y	Y	Y	Y	Y
Individual FE	Y	Y	Y	Y	Y	Y
Baseline Controls	Y	Y	Y	Y	Y	Y
Observations	1,738,727	1,738,727	1,738,727	1,738,727	1,738,727	1,738,727
R-squared	0.401	0.569	0.240	0.285	0.259	0.278

Notes: This table uses the US–China trade war as an exogenous uncertainty shock to the stock market and examines whether the historical climate variability of an investor's hometown affects their trading intensity and tendency to trade risky stocks. The sample is restricted to data from 2017Q1 to 2019Q1. *TradeWar* equals one for all quarters starting from 2018Q3 and zero otherwise. *Hist. Climate Var.* is the standard deviation of prefecture-level PDSI (1500–1950). *VIX* is the quarterly average of the daily SZ50 VIX index minus 10. Controls and specifications follow Table 3. All continuous variables are winsorized at the top and bottom 1% levels. Standard errors are clustered at the investor's hometown city level and are reported in parentheses. *** $p < 0.01$, ** $p < 0.05$, * $p < 0.10$.

Table 8: Historical Climate Variability and Household Risk-Taking

Dep. Var.	(1)	(2)	(3)	(4)	(5)	(6)
	Entrepreneur (0/1)		Fin Debt / Asset		Cash / Asset	
Hist. Climate Var. × *EPU*	-0.0128**	-0.0155*	-10.3315**	-11.5649	0.8267**	1.3624**
	(0.0056)	(0.0083)	(4.9862)	(8.3657)	(0.3914)	(0.5395)
Cont. Climate Var. × *EPU*		0.0041		1.8353		-0.7971
		(0.0078)		(8.4085)		(0.5073)
Household FE	Y	Y	Y	Y	Y	Y
Year FE	Y	Y	Y	Y	Y	Y
Household-level controls	Y	Y	Y	Y	Y	Y
Birth-city controls	Y	Y	Y	Y	Y	Y
Observations	19,061	19,061	19,061	19,061	19,061	19,061
R-squared	0.729	0.729	0.591	0.591	0.653	0.653

Notes: This table examines whether historical climate variability influences households' risk-taking behavior during periods of heightened economic uncertainty, using data from the 2014–2022 waves of the China Family Panel Studies (CFPS). The sample is restricted to households whose registered residence has not changed over time. *Entrepreneur* is a dummy variable that takes the value of one if any household member operates their own business, and zero otherwise; *Fin Debt / Asset* is the ratio of total debt—excluding housing mortgages—to total assets; *Cash / Asset* is cash holdings divided by total assets. *Hist. Climate Var.* is the standard deviation of prefecture-level PDSI from 1500–1950, and *Cont. Climate Var.* is the standard deviation of PDSI from 1950–2000. *EPU* is the average monthly Economic Policy Uncertainty index in the previous year, scaled by 100. Household and year fixed effects are included. Household-level time-varying controls include household total assets, expenditures, income, housing property, family size, a rural-resident dummy, and a house loan-holding dummy, as well as last-year birth-city GDP per capita and GDP growth rate. All continuous variables are winsorized at the top and bottom 1% levels. Standard errors are clustered at the household's birth-city level and are reported in parentheses. *** $p < 0.01$, ** $p < 0.05$, * $p < 0.10$.

Table 9: Historical Climate Variability and Corporate Risk-Taking

Dep. Var.	(1)	(2)	(3)	(4)	(5)	(6)
	R&D		M&A		Idiosyncratic Volatility	
Hist. Climate Var. × *EPU*	-0.2519*	-0.5310***	-0.1391**	-0.0807	-0.0013***	-0.0019***
	(0.1223)	(0.0945)	(0.0356)	(0.0570)	(0.0001)	(0.0004)
Cont. Climate Var. × *EPU*		0.2846**		-0.0595		0.0006
		(0.0977)		(0.0321)		(0.0005)
CEO FE	Y	Y	Y	Y	Y	Y
Firm FE	Y	Y	Y	Y	Y	Y
Year FE	Y	Y	Y	Y	Y	Y
Firm-level controls	Y	Y	Y	Y	Y	Y
Observations	2,436	2,436	2,436	2,436	2,434	2,434
R-squared	0.877	0.877	0.396	0.396	0.635	0.635

Notes: This table examines whether the historical climate variability of a top executive's hometown influences corporate risk-taking behavior. To ensure substantial managerial discretion, the sample is restricted to non-state-owned enterprises (non-SOEs) in which the CEO also serves as board chairman. We employ three proxies for corporate risk-taking: (i) R&D expenditure scaled by lagged total assets, (ii) the annual number of M&A transactions, and (iii) the idiosyncratic volatility of firm stock returns. Due to data availability, the CEO's hometown is identified at the province level. *Hist. Climate Var.* is the standard deviation of prefecture-level PDSI from 1500–1950, and *Cont. Climate Var.* is the standard deviation of PDSI from 1950–2000. *EPU* is the average monthly Economic Policy Uncertainty index in the previous year, scaled by 100. Firm-level control variables include lagged total assets, leverage, cash ratio, ROE, the book-to-market ratio, and stock return. We also control for the squared age of the CEO. All continuous variables are winsorized at the top and bottom 1% levels. Standard errors are clustered at the CEO's hometown-province and industry level and are reported in parentheses. *** $p < 0.01$, ** $p < 0.05$, * $p < 0.10$.

Table 10: Decomposing Climate Variability: Persistent vs. Unpredictable Components

Dep. Var.	(1)	(2)	(3)	(4)	(5)	(6)
	Trading Intensity				Risky Stock Selection	
	BuyMore	*NetTrade*	*NetRatio*		*IvolTilt*	*BetaTilt*	*NonEpTilt*
Persistent Variability × *VIX*	0.0001	-0.0006	0.0281*		0.0009	0.0004	0.0306
	(0.0002)	(0.0031)	(0.0144)		(0.0006)	(0.0004)	(0.0239)
Stochastic Variability × *VIX*	-0.0011***	-0.0136***	-0.0647***		-0.0041***	-0.0017***	-0.1194***
	(0.0003)	(0.0038)	(0.0195)		(0.0008)	(0.0005)	(0.0339)
Individual FE	Y	Y	Y		Y	Y	Y
Quarter FE	Y	Y	Y		Y	Y	Y
Baseline Controls	Y	Y	Y		Y	Y	Y
Observations	7,764,502	7,764,502	7,764,502		7,764,502	7,764,502	7,764,502
R-squared	0.269	0.446	0.109		0.168	0.148	0.157

Notes: This table explores the specific components of historical climate experience that drive the risk-aversion behaviors observed in the baseline results (Tables 3 and 4). Historical climate variability is decomposed using an autoregressive model of order 5 (AR(5)): *Persistent Variability* is the persistent component, captured by the standard deviation of the fitted values, while *Stochastic Variability* is the stochastic component, calculated as the standard deviation of the residuals. The model also controls for *Disaster Freq.*, defined as the frequency of extreme climate events over the 1500–1950 window. A climate disaster is defined at the grid-cell level when $|\text{PDSI}| > 2$; *Disaster Freq.* is the frequency of such observations, scaled by 100. All continuous variables are winsorized at the top and bottom 1% levels. Control variables are the same as in Table 3. Individual and quarter fixed effects are included. Standard errors are clustered at the investor's hometown city level and are reported in parentheses. *** $p < 0.01$, ** $p < 0.05$, * $p < 0.10$.

Table 11: Migration Subsample Tests: Birth City vs Living City

Dep. Var.	(1)	(2)	(3)	(4)	(5)	(6)
	Trading Intensity			Risky Stock Selection		
	BuyMore	*NetTrade*	*NetRatio*	*IvolTilt*	*BetaTilt*	*NonEpTilt*
Hist. Climate Var. × VIX	-0.0005	-0.0167***	-0.0532***	-0.0035***	-0.0012***	-0.0751*
	(0.0003)	(0.0062)	(0.0130)	(0.0009)	(0.0004)	(0.0409)
Cont. Climate Var. × VIX	0.0004	0.0081*	0.0619**	0.0026**	0.0011**	0.0680
	(0.0004)	(0.0047)	(0.0256)	(0.0012)	(0.0006)	(0.0514)
Hist. Climate Var. (Living City) × VIX	0.0003	0.0000	0.0489	0.0028**	0.0011	0.0226
	(0.0004)	(0.0076)	(0.0367)	(0.0012)	(0.0009)	(0.0543)
Cont. Climate Var. (Living City) × VIX	-0.0010**	-0.0082	-0.1026**	-0.0053***	-0.0023**	-0.1008*
	(0.0005)	(0.0069)	(0.0398)	(0.0013)	(0.0009)	(0.0581)
Baseline Controls	Y	Y	Y	Y	Y	Y
Individual FE	Y	Y	Y	Y	Y	Y
Quarter FE	Y	Y	Y	Y	Y	Y
Observations	1,409,413	1,409,413	1,409,413	1,409,413	1,409,413	1,409,413
R-squared	0.270	0.441	0.114	0.173	0.150	0.159

Notes: This table replicates the baseline tests in Tables 3 and 4 using a subsample restricted to investors residing in a city different from their birth city. *Hist. Climate Var.* is the standard deviation of prefecture-level PDSI (1500–1950), and *Cont. Climate Var.* is the standard deviation of PDSI (1950–2000); we construct both variables for the investor's birth city and, separately, for their current city of residence (denoted "Living City" in the row labels). *VIX* is the quarterly average of the daily SZ50 VIX index minus 10. All other variables and model specifications follow Tables 3 and 4. All continuous variables are winsorized at the top and bottom 1% levels. Individual and quarter fixed effects are included, and control variables are the same as in Table 3. Standard errors are clustered at the investor's birth-city level and are reported in parentheses. *** $p < 0.01$, ** $p < 0.05$, * $p < 0.10$.

Table 12: Historical Persistence: Climatic Variability and Cash Crop Adoption

Dep. Var.	(1) Cotton	(2) Foreign Cotton	(3) Foreign Cotton	(4) Cotton	(5) Foreign Cotton	(6) Foreign Cotton
Hist. Climate Var.	-0.183**	-0.177***	-0.201*	-0.165***	-0.158***	-0.193*
	(0.044)	(0.041)	(0.105)	(0.044)	(0.041)	(0.103)
Relative Soil Suitability (cotton vs staple)	1.692***	2.081***	0.102			
	(0.384)	(0.338)	(1.220)			
Cotton Soil Suitability				0.001***	0.001***	0.0001
				(0.000)	(0.000)	(0.001)
Sample	China proper	China proper	Cotton-growing Region	China proper	China proper	Cotton-growing Region
province FE	Y	Y	Y	Y	Y	Y
county-level characteristics	Y	Y	Y	Y	Y	Y
Observation	1583	1583	325	1583	1583	325
R-squared	0.32	0.286	0.593	0.332	0.3	0.593

Note: This table explores whether historical climate variability influenced risk-taking behavior in historical contexts. We use cash crop adoption as a proxy for risk-taking in historical agricultural production, and the results indicate that regions with higher historical climate variability were less likely to cultivate cash crops (e.g., cotton). Using a county-level dataset, the outcome variable measures cash crop adoption in the 1930s. Columns (1) and (4) use a binary indicator of whether a county grew cotton as a proxy for risky agricultural practice. Columns (2), (3), (5), and (6) restrict the sample to cotton-growing counties and use the adoption of the American cotton variety (a new, higher-risk cash crop) as the outcome. *Hist. Climate Var.* is the standard deviation of prefecture-level PDSI from 1500–1900, ensuring it precedes the cotton cultivation data. The specifications control for the relative soil suitability of cotton versus staple crops (rice and wheat). Additional control variables include a battery of geo-economic characteristics at city level: land area, ruggedness, coastal status, distance to the Yangtze River, soil suitability for staple crops, quotas for entry-level civil service exams, and provincial capital status. Standard errors are clustered at the county level and are reported in parentheses. *** $p < 0.01$, ** $p < 0.05$, * $p < 0.10$.

Online Appendix

A. Background and Data

- Figure A.1. Spatial Resolution of Climatic Data
- Figure A.2. Spatial Distribution of Climate Variability Measures
- Figure A.3. Distribution Functions of Different Climate Variability Measures
- Figure A.4. Correlation of Historical and Contemporaneous Climate Variability
- Figure A.5. Decomposing Climate Variability: Stochastic vs. Persistent Components
- Figure A.6. Verifying MADA Data Quality
- Figure A.7. Distribution of Risk Preferences in High- vs. Low-Variability Regions
- Figure A.8. Retail Investor Sample Coverage
- Figure A.9. Historical Migration Cost

B. Additional Analysis for Section IV

- Table B.1. Historical Climate Variability and City-Level Characteristics
- Table B.2. Robustness: Alternative Measure for Climate Variability
- Table B.3. Robustness: Value-based Measures of Trading Intensity and Risky Stock Selection
- Table B.4. Robustness: Trading Density
- Table B.5. Robustness: Further Control Geographic Features
- Table B.6. Robustness: Subsample with High MADA Data Quality
- Table B.7. Robustness: Subsample Analysis (Migration-Constrained and Coastal Cities)

C. Additional Analysis for Section V

- Table C.1. Summary Statistics for Table 8 using CFPS
- Table C.2. Summary Statistics for Table 9 using CSMAR
- Table C.3. Robustness: Alternative Measure for Climate Variability

Appendix A: Background and Data

A1. Data on Historical Climate Variability

We use historical climate data to distinguish regions with systematically higher climate risks in the past from those with lower climate risks. Our primary climate variables are sourced from the Monsoon Asia Drought Atlas (MADA) (Cook et al., 2010). MADA relies on paleoclimatic reconstructions, which are derived through sophisticated methods using multiple proxies such as tree rings, ice cores, and corals. It draws from over 300 tree-ring sites across Monsoon Asia and provides estimates of the summer (June–August) Palmer Drought Severity Index. MADA offers long time periods (spanning back to 1500) with a spatial resolution of $2.5^\circ \times 2.5^\circ$. Mada data in fact could go back to 1300, while the tree ring sites are smaller than the samle going back to 1500, so in this paper, we choose constrain our data to 1500 with larger coverage. In this section, we provide more information on our climate variability measures.

We employ two complementary measures of long-term climatic varability. Our primary measure is the standard deviation of the summer Palmer Drought Severity Index (PDSI) between 1500 and 1950, which captures the magnitude of year-to-year variability and is widely used in the literature. As a robustness measure, we use the frequency of weather disasters, defined as the number of years with $|PDSI| > 2$. In the main text (Section 6.1) we further decompose historical climate variability into a persistent and a stochastic component to isolate the role of unpredictability.

For each measure, we construct two versions: one over the historical period 1500–1950 and one over the contemporary period 1950–2000. Since all sampled individuals in our modern data were born after 1950, the historical version captures climate conditions faced by their ancestors and is pre-determined relative to anyone in the sample, while the contemporary version captures climate conditions experienced during their own lifetimes. This separation lets us isolate the long-run cultural channel, transmitted across generations, from any direct lifetime-experience effect, and motivates the placebo test in the main text.

Figure A.1 illustrates the spatial resolution of our climate data and its mapping to modern Chinese prefectures. Because individuals' hometowns are identified at the prefecture level, we aggregate grid-level PDSI to prefecture boundaries using area-weighted zonal statistics. Panel (a) overlays the MADA grid on an example prefecture; Panel (b) confirms the seasonal relevance of the index: based on FAO–GAEZ data, the rice growing season spans roughly June–September, so the summer (June–August) PDSI captures the critical growth period for China's staple crops.

Figure A.2 maps the spatial distribution of historical climate variability across Chinese prefectures using our two measures: the standard deviation of PDSI (Panel a) and the frequency of weather disasters (Panel b). The two measures display highly consistent geographic patterns, with greater historical variability in northern and northwestern China and lower variability in the south. Notably, this spatial distribution does not align with China's economic development pattern (the wealthy southeast versus the interior).

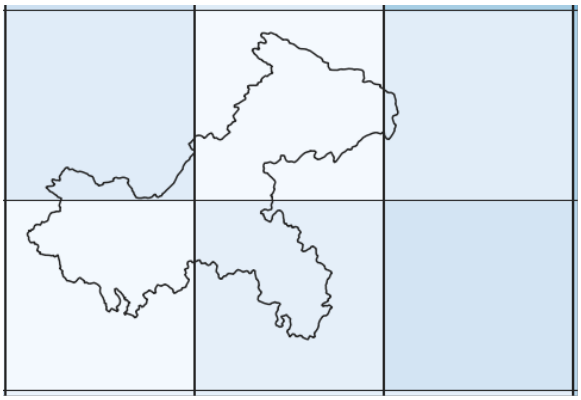
Figure A.3 presents the distribution functions of these two measures across prefectures; both are right-skewed, with most prefectures exhibiting moderate variability and a long tail of high-variability regions. The two measures are also very strongly correlated across pre-

fectures, confirming that our results are not sensitive to the particular measure of historical climate variability used.

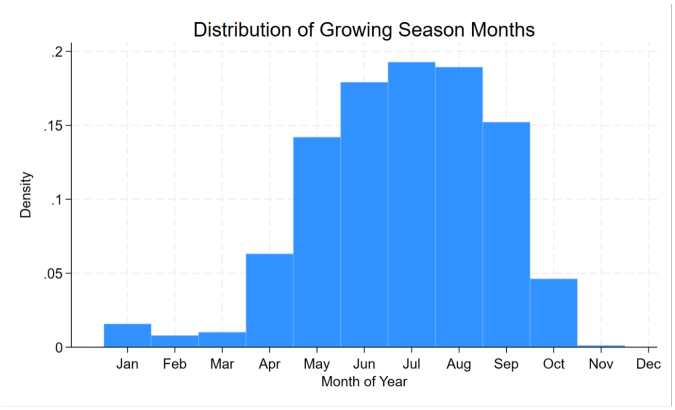
Figure A.4 plots historical (1500–1950) against contemporary (1950–2000) climate variability, for both the standard-deviation measure (Panel a) and the disaster-frequency measure (Panel b). Regional variability is strongly correlated across the two eras, as expected when climatic conditions are largely determined by stable geographic features. This persistence motivates the placebo test using contemporary variability in the main text.

Figure A.5 decomposes historical climate variability into a persistent and a stochastic component using an AR(5) model fitted at each prefecture. At each prefecture, we regress the summer PDSI on its own first five lags. The fitted values capture the part of climate variability that is predictable from recent history, reflecting persistent regimes such as multi-year droughts and slow-moving monsoonal cycles. We define the persistent component as the standard deviation of these fitted values (Panel a). The residuals capture the part that is not predictable from the recent past, the year-to-year shocks that leave little room for ex-ante adaptation. We define the stochastic component as the standard deviation of these residuals (Panel b). The two spatial patterns are related but do not completely overlap, indicating that the persistent and stochastic dimensions of climate variability capture distinct sources of historical risk.

Figure A.1: Spatial Resolution of Climatic Data



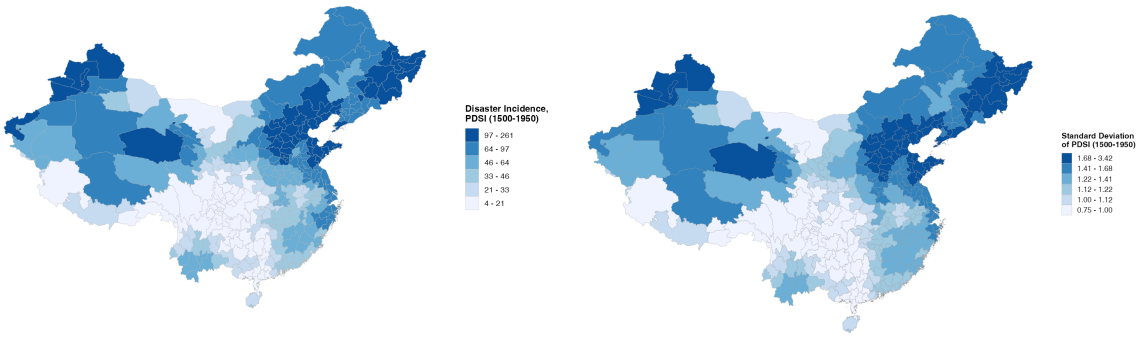
a. Example of Chongqing prefecture on MADA grid



b. Distribution of growing season months for rice. Source: FAO GAEZ.

Notes: As discussed in Section 3.1, we aggregate the summer (June–August) gridded Palmer Drought Severity Index (PDSI) values from the Monsoon Asia Drought Atlas (MADA; Cook et al., 2010). The MADA provides a high-resolution reconstruction of Asian hydroclimate from 1300–2005, with grid cells of 2.5 degrees (approximately 278 km at the equator). We use GIS zonal statistics to aggregate these grids to China's prefecture boundaries. Panel A illustrates the mapping of MADA grid cells to a single Chinese prefecture. Panel B shows that the rice growing season typically runs from June to September (FAO-GAEZ), so the MADA summer PDSI captures the critical period for China's major staple crops.

Figure A.2: Spatial Distribution of Climate Variability Measures

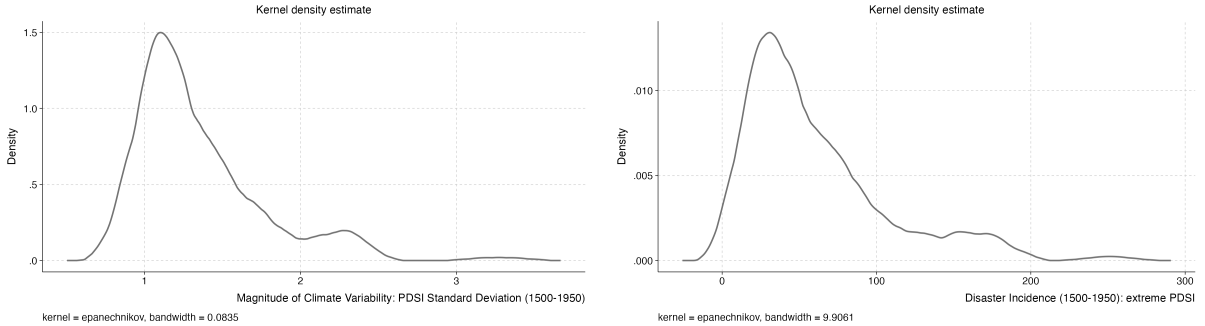


(a) Standard deviation of PDSI (1500–1950)

(b) Frequency of weather disasters, $|PDSI| > 2$ (1500–1950)

Notes: This figure maps historical climate variability across Chinese prefectures (1500–1950) using our two measures: Panel (a) the standard deviation of the summer Palmer Drought Severity Index (PDSI), and Panel (b) the frequency of weather disasters (years with $|PDSI| > 2$). Climate variability is constructed at the MADA grid level and aggregated to modern prefecture boundaries using area-weighted zonal statistics. The two measures display highly consistent geographic patterns.

Figure A.3: Distribution Functions of Different Climate Variability Measures

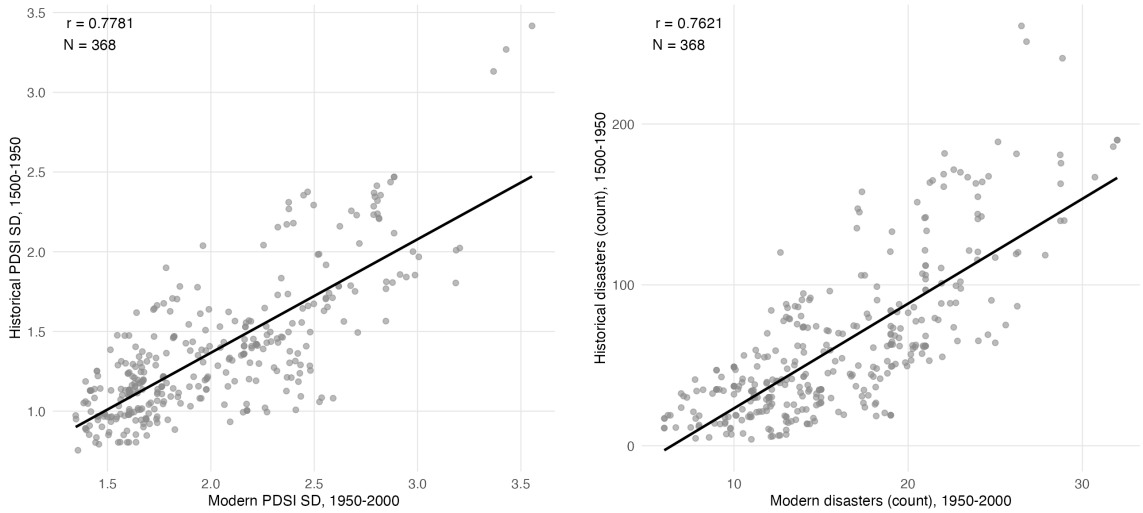


(a) Standard deviation of PDSI (1500–1950)

(b) Frequency of weather disasters, $|PDSI| > 2$ (1500–1950)

Notes: This figure shows the kernel density (distribution function) of our two historical climate variability measures across Chinese prefectures (1500–1950): Panel (a) the standard deviation of PDSI, and Panel (b) the frequency of weather disasters ($|PDSI| > 2$). Both measures are right-skewed, with most prefectures exhibiting moderate variability and a long tail of high-variability regions. Kernel = Epanechnikov.

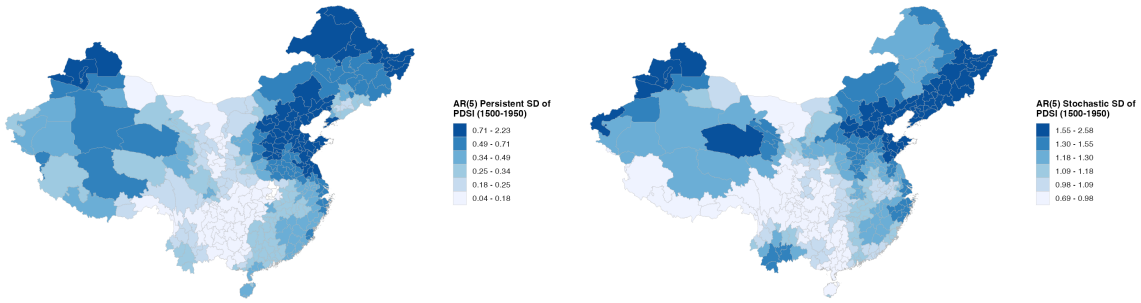
Figure A.4: Correlation of Historical and Contemporaneous Climate Variability



(a) Standard deviation of PDSI: 1500–1950 vs. (b) Disaster frequency: 1500–1950 vs. 1950–2000
1950–2000

Notes: Each panel plots historical (1500–1950) against contemporary (1950–2000) climate variability across 368 prefectures, with the OLS fit. Panel (a) uses the standard deviation of PDSI; Panel (b) uses the frequency of weather disasters. Since all sampled individuals in our modern data were born after 1950, the historical version captures climate conditions faced by their ancestors and is pre-determined relative to anyone in the sample, while the contemporary version captures climate conditions experienced during their own lifetimes. Regional variability is strongly correlated across the two eras, consistent with climatic conditions being largely determined by stable geographic features; this motivates the placebo test using contemporary variability in the main text.

Figure A.5: Decomposing Climate Variability into Stochastic and Persistent Components



(a) Persistent component: SD of AR(5) fitted values

(b) Stochastic component: SD of AR(5) residuals

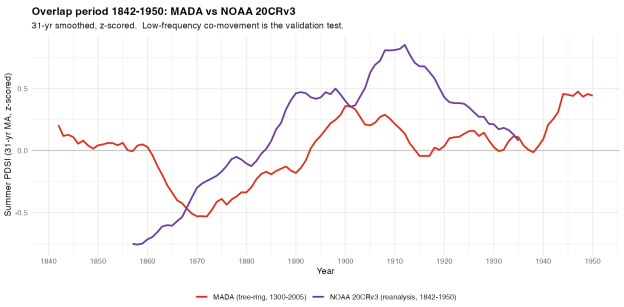
Notes: This figure maps the two components of historical climate variability (1500–1950) obtained from an AR(5) decomposition of the summer PDSI series at each prefecture. Panel (a) shows the persistent (predictable) component, computed as the standard deviation of the fitted values; Panel (b) shows the stochastic (unpredictable) component, computed as the standard deviation of the residuals. The two spatial patterns are related but do not completely overlap, indicating that the two components capture distinct dimensions of historical climate risk.

A2. Quality of the MADA.
MADA's reconstruction quality is well-established. Cook et al. (2010) reports substantial cross-validation skill against instrumental records across the grid cells used in our analysis, with positive reduction-of-error and coefficient-of-efficiency statistics throughout the spatial domain. We further provide two checks to further verify the quality of MADA data in our setting.

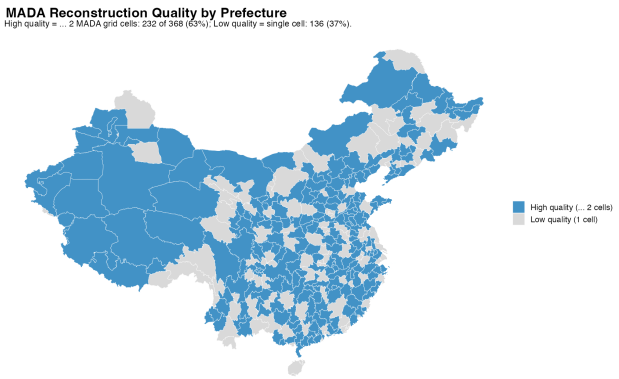
First, we compare MADA against the NOAA 20th Century Reanalysis (20CR), a fully independent climate dataset. Unlike MADA, which reconstructs climate from tree-ring proxies, 20CR is a model-based reanalysis that assimilates surface pressure observations into a general-circulation model; the two sources rest on different inputs and different methodologies, sharing only the climate signal they aim to recover. MADA also extends much further back in time, beginning in 1300 versus 1842 for 20CR. Figure A.6 plots the two series across their overlap window, 1842–1950, as 31-year moving averages, z-scored so the comparison emphasises low-frequency co-movement (the relevant validation test for the multi-century variability we use). The two reconstructions recover a similar long-run pattern despite sharing no common inputs, indicating that MADA captures genuine climate variation rather than tree-ring artefacts.

Second, MADA reconstruction quality varies geographically with the density of tree-ring sites contributing to each grid cell. Prefectures whose polygons overlap multiple MADA grid cells yield a more precisely reconstructed climate series than prefectures supported by a single cell. Figure A.7 maps this density across our sample: 232 of 368 prefectures (63%) are high-quality (at least two contributing cells), while 136 (37%) are low-quality (a single contributing cell). To address the concern that reconstruction noise in low-density prefectures might drive our results, we replicate our main analysis on the high-quality subsample. The results, reported in Appendix Table B.6, are robust in both sign and magnitude, indicating that local MADA quality does not drive our findings.

Figure A.6: Verifying MADA Data Quality



(a) Comparing MADA with NOAA 20CRv3 (1842–1950 overlap)



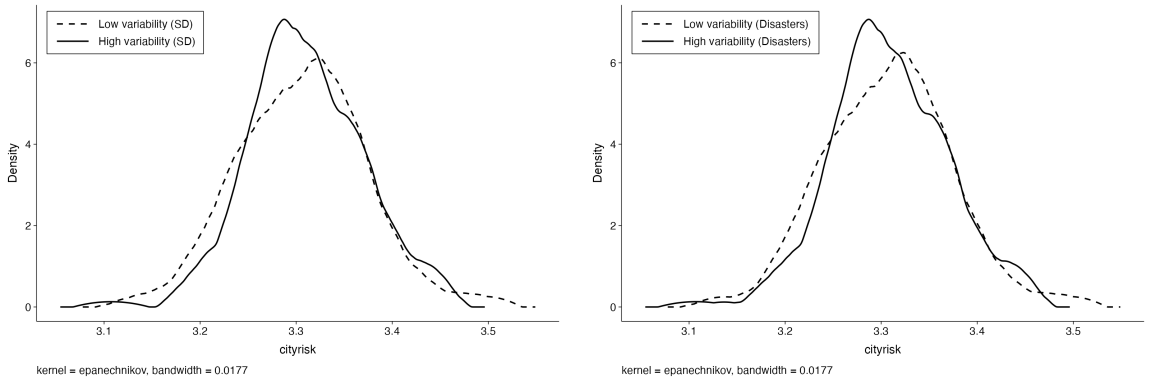
(b) Spatial distribution of MADA reconstruction quality

Notes: This figure presents two validations of the MADA reconstruction. Panel (a) compares the China-average summer (June–August) PDSI from MADA (red) against the NOAA 20th Century Reanalysis Version 3 (20CRv3, purple) across their 1842–1950 overlap window. Both series are 31-year moving averages and z-scored, so the comparison emphasises low-frequency co-movement, which is the relevant validation test given that our identification uses multi-century climate variability. MADA is a tree-ring paleoclimatic reconstruction; 20CRv3 is a model-based reanalysis that assimilates surface pressure observations into a general-circulation atmospheric model. The two sources share no common inputs, yet they recover a similar long-run climate pattern, supporting MADA's external validity. Panel (b) maps MADA reconstruction quality across Chinese prefectures, defined by the number of MADA grid cells contributing to each prefecture polygon. High-quality prefectures (dark blue, 232 of 368) overlap at least two MADA grid cells, so the aggregated PDSI series reflects genuine spatial averaging rather than a single-cell reconstruction. Low-quality prefectures (light grey, 136 of 368) are supported by only one grid cell. The high-quality subsample is used in the robustness check reported in Appendix Table B.6.

A3. Historical Climate Variability and Risk Preference

As motivational evidence, in Figure A.6 we examine the relationship between elicited risk tolerance and historical climate variability. The figure displays the kernel density of investors' risk-tolerance scores (higher values indicate greater tolerance), with prefectures split at the median of each of our two climate measures: the standard deviation of PDSI (Panel a) and the frequency of weather disasters (Panel b), both over 1500–1950. Both panels reveal a clear distributional shift: high-variability regions exhibit lower risk tolerance than their more stable counterparts.

Figure A.7: Distribution of Risk Preferences in High- vs. Low-Variability Regions



(a) Split at median SD of PDSI (1500–1950)

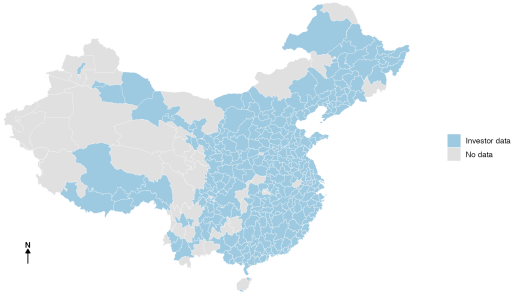
(b) Split at median disaster frequency (1500–1950)

Notes: This figure plots the kernel density of investors' elicited risk-tolerance scores (higher = greater tolerance) across the 294 sampled prefectures. Prefectures are split at the median of each historical climate variability measure (1500–1950): Panel (a) the standard deviation of PDSI; Panel (b) the frequency of weather disasters ($|PDSI| > 2$). The dashed line shows the low-variability cohort and the solid line the high-variability cohort. Both panels show a clear distributional shift: high-variability regions exhibit lower risk tolerance than their more stable counterparts. Kernel = Epanechnikov.

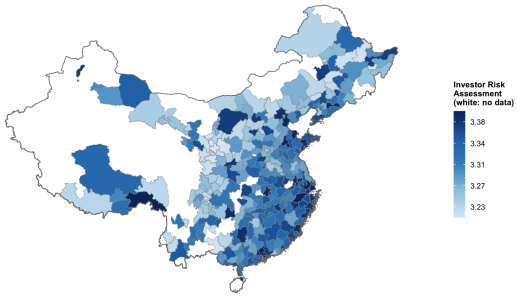
A4. Retail Investor Sample Coverage

Figure A.7 summarizes the geographic coverage and within-sample variation of our primary individual-investor sample. Panel (a) shades each modern prefecture by whether we observe at least one sampled investor whose registered hometown is located there: the sample spans 294 of 368 modern Chinese prefectures, with near-complete coverage within China proper, the eighteen interior provinces that historically account for roughly 80% of the national population. The unsampled prefectures are overwhelmingly small, sparsely populated units in peripheral frontier regions (e.g., Tibet, Qinghai, southern Xinjiang, and parts of Inner Mongolia and Gansu), representing a negligible share of the national population and of stock-market participation. Panels (b)–(d) restrict attention to the 294 sampled prefectures and confirm substantial cross-prefecture variation in the variables driving our identification: (b) the city-level risk-tolerance assessment, (c) the standard deviation of PDSI from 1500–1950, and (d) the frequency of extreme weather shocks ($|\text{PDSI}| > 2$) from 1500–1950.

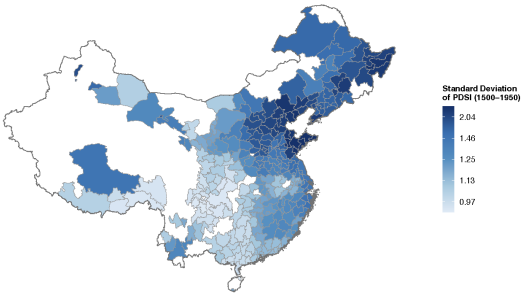
Figure A.8: Retail Investor Sample Coverage and Within-Sample Variation



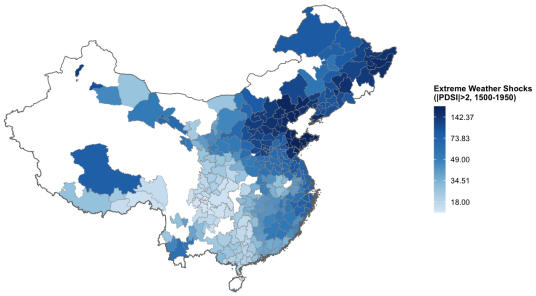
(a) Sample coverage (294 of 368 cities)



(b) Risk-tolerance assessment



(c) SD of PDSI (1500–1950)



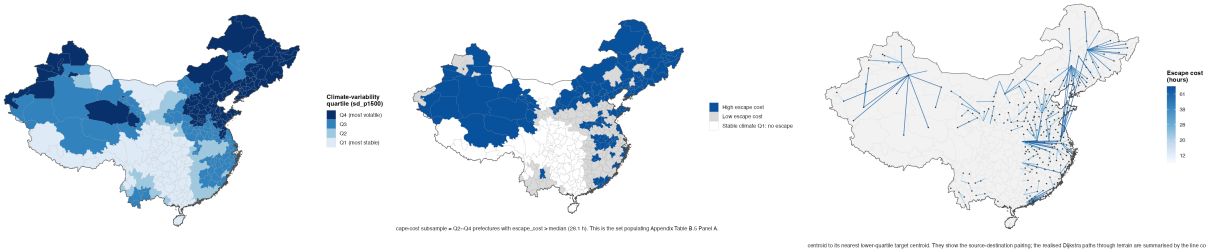
(d) Extreme weather shocks ($|\text{PDSI}| > 2$, 1500–1950)

Notes: This figure summarises our retail investor sample. Panel (a) shows the geographic coverage of the brokerage data: prefectures shaded in blue are those for which we observe at least one sampled investor (294 of 368 modern Chinese prefectures); prefectures in grey have no sampled investors. Coverage is near-complete within China proper, the eighteen interior provinces that historically account for more than 80% of the Chinese population, and the unsampled units are overwhelmingly small, sparsely populated peripheral-frontier prefectures. Panels (b)–(d) restrict attention to the 294 sampled prefectures: Panel (b) maps the city-level risk-tolerance assessment, Panel (c) maps the standard deviation of PDSI from 1500–1950, and Panel (d) maps the frequency of extreme weather shocks ($|\text{PDSI}| > 2$) from 1500–1950. The colour scales in Panels (b)–(d) are percentile-stretched within the sampled subset; legend labels report actual values at the 10th, 30th, 50th, 70th, and 90th percentiles. The panels show substantial cross-prefecture variation in both climate measures and risk tolerance within the sampled subset.

A5. Construction of the Historical Escape-Cost Measure.
The escape cost is a terrain-adjusted walking-time distance from each prefecture to the nearest prefecture in a lower climate-variability quartile. We build a five arc-minute (≈ 9 km) cost raster of China. At each cell, slope is computed from the SRTM DEM and converted to walking speed via the Tobler function, $v = 6 \cdot \exp(-3.5\,|\tan\theta + 0.05|)$ km/h. Ocean and lakes larger than 10 km^2 (HydroLAKES) are impassable. Cells above 4,000 m carry a $2\times$ penalty for altitude; cells along major river corridors (HydroRIVERS, Strahler order ≥ 5) carry a $0.3\times$ discount for water transport. Prefectures are split into quartiles of $sd_{1500\text{–}1950}$ (Q1 = most stable). For each Q2–Q4 prefecture we solve Dijkstra's shortest path on the cost raster from the prefecture centroid to the nearest centroid in a strictly lower quartile, and take the cumulative walking time, in hours, as the escape cost.

Figure A.9 illustrates this construction across three panels. We will use the resulting measure in Appendix Table B.7, Panel A, where the baseline trading specifications are re-estimated on the migration-constrained subsample. Historical out-migration from these prefectures was sufficiently costly that selective sorting of more risk-tolerant ancestors is implausible, so a coefficient that is similar in sign and magnitude to the full-sample estimate is evidence that the relationship between historical climate variability and modern risk-taking is not generated by selective ancestral migration.

Figure A.9: Historical Migration Cost



(a) Climate-variability quartile (Q1 = most stable, Q4 = most volatile)

(b) High escape-cost subsample

(c) Source-to-destination escape routes (coloured by escape cost in hours)

Notes: This figure summarises the historical migration cost that constrained selective out-migration from high-variability prefectures. **Panel (a)** shows the cross-prefecture distribution of climate variability, partitioned into quartiles of the standard deviation of summer PDSI over 1500–1950 (Q1 = most stable, Q4 = most volatile). The escape-cost variable is defined as the cost of reaching a strictly lower quartile, so this panel establishes the set of source prefectures (Q2–Q4) and the set of admissible destinations (any strictly lower quartile). **Panel (b)** shows the migration-constrained subsample used in the robustness test in Appendix Table B.7, Panel A: Q2–Q4 prefectures with escape cost above the Q2–Q4 median (28.1 hours) are shown in dark blue ("High escape cost"); Q2–Q4 prefectures at or below the median are shown in light grey ("Low escape cost"); and Q1 prefectures, which have no lower quartile to escape to, are shown in white ("Stable climate Q1: no escape"). **Panel (c)** shows the source–destination pairings for the 276 Q2–Q4 prefectures: each line connects a source prefecture's centroid to the centroid of its nearest lower-quartile destination, with the line colour encoding the realised escape cost (hours of Dijkstra least-cost walking time on the terrain raster; see Section A5 for the construction of the cost surface).

B: Additional Analysis for Section IV

Table B.1: Historical Climate Variability and City-Level Characteristics

	Historical Climate Variability		
	(1)	(2)	(3)
Nightlight Intensity (2024)	0.001	0.001	-0.001
	(0.716)	(0.808)	(-0.413)
Provincial Capital	-0.048	-0.060*	-0.046
	(-1.259)	(-1.684)	(-1.099)
Distance to Yangtze River	-0.014*	-0.018**	-0.031***
	(-1.921)	(-2.348)	(-2.713)
Coastal Region	0.249***	0.231***	0.153***
	(4.291)	(3.889)	(3.086)
Latitude	0.047***	0.043***	0.037***
	(4.436)	(3.666)	(3.809)
Longitude	0.007	0.012	-0.010
	(0.923)	(1.429)	(-1.232)
Log(Area)	-0.000	-0.000	-0.000
	(-0.252)	(-0.159)	(-0.015)
Elevation	0.000	0.000	-0.000***
	(0.305)	(0.853)	(-3.686)
Soil Suitability for Rice	0.000	0.000	-0.000
	(0.855)	(1.269)	(-1.270)
Soil Suitability for Wheat	0.000	0.000	0.000
	(0.840)	(1.254)	(1.391)
Constant	-1.091	-1.598*	1.925**
	(-1.347)	(-1.878)	(2.373)
Observations	368	368	368
R-squared	0.796	0.787	0.814

Notes: This table shows that the treatment variable—historical climate variability—is not correlated with indicators of current economic development (e.g., 2024 night light intensity), proxies for historical agricultural intensity (e.g., soil suitability for staple crops), and measures of regional governance quality (e.g., provincial capital status). As expected, some geographic features (e.g., proximity to the coastline, latitude, and elevation) are associated with historical climate variability. Coastal or high-latitude regions naturally experience different weather patterns, but we address potential confounding by including city or individual fixed effects in all specifications, which absorb time-invariant city-level characteristics (e.g., geography). Standard errors are clustered at the birth city level and are reported in parentheses. *** $p < 0.01$, ** $p < 0.05$, * $p < 0.10$.

Table B.2: Robustness: Alternative Measure for Climate Variability

Dep. Var.	(1)	(2)	(3)	(4)	(5)	(6)
	Trading Intensity			Risky Stock Selection		
	BuyMore	*NetTrade*	*NetRatio*	*IvolTilt*	*BetaTilt*	*NonEpTilt*
Extreme Weather Shocks× *VIX*	-0.0006***	-0.0087***	-0.0205***	-0.0019***	-0.0007***	-0.0519***
	(0.0001)	(0.0014)	(0.0068)	(0.0003)	(0.0002)	(0.0114)
Baseline Controls	Y	Y	Y	Y	Y	Y
Individual FE	Y	Y	Y	Y	Y	Y
Quarter FE	Y	Y	Y	Y	Y	Y
Observations	7,764,502	7,764,502	7,764,502	7,764,502	7,764,502	7,764,502
R-squared	0.269	0.446	0.109	0.168	0.148	0.157

Note: This table replicates Tables 3 and 4 in the main paper, but instead of our primary measure of climate variability (the standard deviation of PDSI), it uses the total number of extreme weather events over 1500–1950, defined as years with |PDSI| $>$ 2. All other variables and model specifications follow Tables 3 and 4. All continuous variables are winsorized at the top and bottom 1% levels. Individual- and quarter-fixed effects are included. Standard errors are clustered at the investor's hometown city level and are reported in parentheses. *** $p < 0.01$, ** $p < 0.05$, * $p < 0.10$.

Table B.3: Robustness: Value-based Measures of Trading Intensity and Risky Stock Selection

Dep. Var.	(1)	(2)	(3)	(4)	(5)	(6)
	Trading Intensity			Risky Stock Selection		
	BuyMore	*NetTrade*	*NetRatio*	*IvolTilt*	*BetaTilt*	*NonEpTilt*
Hist. Climate Var.× VIX	-0.0007***	-57.8656**	-0.0183***	-0.0011***	-0.0004***	-0.0278***
	(0.0002)	(24.7621)	(0.0065)	(0.0003)	(0.0001)	(0.0063)
Individual FE	Y	Y	Y	Y	Y	Y
Individual trading controls	Y	Y	Y	Y	Y	Y
Quarter FE	Y	Y	Y	Y	Y	Y
Observations	7,764,502	7,764,502	7,764,502	7,764,502	7,764,502	7,764,502
R-squared	0.154	0.062	0.069			

Note: This table replicates the baseline tests in Table 3 and Table 4 but replaces all trade number-based measures with their value-based counterparts. Columns (1)–(3) report value-based trading-intensity outcomes: *BuyMore* equals one if the value of buy trades exceeds that of sell trades, *NetTrade* is the difference between the value of buy and sell trades, and *NetRatio* is *NetTrade* divided by total trading value. Columns (4)–(6) report value-based risky-stock-selection tilts (*IvolTilt*, *BetaTilt*, *NonEpTilt*). *Hist. Climate Var.* is the standard deviation of prefecture-level PDSI (1500–1950). *VIX* is the quarterly average of the daily SZ50 VIX index minus 10. All columns use the full-controls specification (individual and quarter fixed effects plus individual trading controls); all other variables and model specifications follow Table 3 and Table 4. All continuous variables are winsorized at the top and bottom 1% levels. Standard errors are clustered at the investor's hometown city level and are reported in parentheses. *** $p < 0.01$, ** $p < 0.05$, * $p < 0.10$.

Table B.4: Robustness: Trading Density

Dep. Var.	(1) *Trade*	(2) *TotalTrade*	(3) *TotalValue*	(4) *Turnover*
Hist. Climate Var.× VIX	-0.0009***	-0.0837***	-2,565.2863***	-1.2555*
	(0.0002)	(0.0119)	(399.6508)	(0.7573)
Baseline Controls	Y	Y	Y	Y
Individual FE	Y	Y	Y	Y
Quarter FE	Y	Y	Y	Y
Observations	7,764,502	7,764,502	10,403,820	10,094,477
R-squared	0.401	0.699	0.665	0.438

Note: This table examines whether the historical climate variability of an investor's hometown affects risk-taking, captured by value-based trading density measures, during periods of heightened market uncertainty. *Trade* equals one if the investor has traded in the quarter. *TotalTrade* is the sum of the number of buy and sell trades. *TotalValue* is the sum of buy and sell value. *Turnover* is *TotalValue* scaled by the investor's maximum account balance in last quarter. The model specification and definition of other variables are the same as in column (3) of Table 3. All continuous variables are winsorized at the top and bottom 1% levels. Individual- and quarter-fixed effects are included. Standard errors are clustered at the investor's hometown city level and are reported in parentheses. *** $p < 0.01$, ** $p < 0.05$, * $p < 0.10$.

Table B.5: Robustness: Further Control for Geographic Features

Dep. Var.	(1)	(2)	(3)	(4)	(5)	(6)
	Trading Intensity			Risky Stock Selection		
	BuyMore	*NetTrade*	*NetRatio*	*IvolTilt*	*BetaTilt*	*NonEpTilt*
Hist. Climate Var × VIX	-0.0004**	-0.0078***	-0.0200	-0.0012**	-0.0007**	-0.0368*
	(0.0002)	(0.0029)	(0.0132)	(0.0006)	(0.0003)	(0.0210)
Baseline Controls	Y	Y	Y	Y	Y	Y
Individual FE	Y	Y	Y	Y	Y	Y
Quarter FE	Y	Y	Y	Y	Y	Y
Geo×Quarter FE	Y	Y	Y	Y	Y	Y
Observations	7,764,502	7,764,502	7,764,502	7,764,502	7,764,502	7,764,502
R-squared	0.269	0.446	0.110	0.168	0.148	0.157

Note: This table replicates the baseline trading tests in Tables 3 and 4 while adding fixed effects that allow birth-city geographic features to have time-varying effects. We interact a battery of birth-city geographic characteristics (latitude, longitude, elevation, coastal status, land area, and major-river access) with quarter fixed effects, so that any differential response to market uncertainty associated with birth-region geography is absorbed. *Hist. Climate Var.* is the standard deviation of prefecture-level PDSI (1500–1950); *VIX* is the quarterly average of the daily SZ50 VIX index minus 10. The coefficient on *Hist. Climate Var.* × VIX remains negative and comparable in magnitude to the baseline estimates, indicating that the effect is not driven by birth-region geography. All other variables and model specifications follow Tables 3 and 4. All continuous variables are winsorized at the top and bottom 1% levels. Standard errors are clustered at the investor's hometown city level and are reported in parentheses. *** $p < 0.01$, ** $p < 0.05$, * $p < 0.10$.

Table B.6: Robustness: Subsample with High MADA Data Quality

Dep. Var.	(1)	(2)	(3)	(4)	(5)	(6)
	Trading Intensity			Risky Stock Selection		
	BuyMore	*NetTrade*	*NetRatio*	*IvolTilt*	*BetaTilt*	*NonEpTilt*
Hist. Climate Var.× VIX	-0.0007***	-0.0097***	-0.0230***	-0.0021***	-0.0009***	-0.0553***
	(0.0001)	(0.0018)	(0.0083)	(0.0004)	(0.0002)	(0.0142)
Baseline Controls	Y	Y	Y	Y	Y	Y
Individual Trading Controls	Y	Y	Y	Y	Y	Y
Individual FE	Y	Y	Y	Y	Y	Y
Quarter FE	Y	Y	Y	Y	Y	Y
Observations	5,162,562	5,162,562	5,162,562	5,162,562	5,162,562	5,162,562
R-squared	0.269	0.446	0.109	0.168	0.148	0.157

Note: This table replicates the baseline trading tests in Tables 3 and 4, restricting the sample to investors whose birth city has higher-quality MADA reconstruction data. A prefecture is treated as high-quality when its polygon contains at least two valid MADA grid cells, so that the aggregated PDSI series reflects genuine spatial averaging rather than a single-cell reconstruction. The dependent variables are the three trading-intensity measures (*BuyMore*, *NetTrade*, *NetRatio*) and the three risky-stock-selection tilts (*IvolTilt*, *BetaTilt*, *NonEpTilt*). *Hist. Climate Var.* is the standard deviation of prefecture-level PDSI (1500–1950); *VIX* is the quarterly average of the daily SZ50 VIX index minus 10. The coefficient on *Hist. Climate Var.* × VIX remains negative and statistically significant across all six outcomes and comparable in magnitude to the full-sample estimates, indicating that local MADA reconstruction quality does not drive our findings. All other variables and model specifications follow Tables 3 and 4. All continuous variables are winsorized at the top and bottom 1% levels. Standard errors are clustered at the investor's hometown city level and are reported in parentheses. *** $p < 0.01$, ** $p < 0.05$, * $p < 0.10$.

Table B.7: Robustness: Subsample Analysis (Migration-Constrained and Coastal Cities)

Panel A: Cities with High Historical Migration Difficulty

	(1) *BuyMore*	(2) *NetTrade*	(3) *NetRatio*	(4) *IvolTilt*	(5) *BetaTilt*	(6) *NonEpTilt*
ClimateVarHis× *VIX*	-0.0005***	-0.0076***	-0.0197*	-0.0014**	-0.0009***	-0.0458***
	(0.0002)	(0.0026)	(0.0116)	(0.0005)	(0.0003)	(0.0172)
Controls	Y	Y	Y	Y	Y	Y
Client FE	Y	Y	Y	Y	Y	Y
Quarter FE	Y	Y	Y	Y	Y	Y
Observations	2,021,657	2,021,657	2,021,657	2,021,657	2,021,657	2,021,657
R-squared	0.268	0.443	0.109	0.165	0.146	0.155

Panel B: Coastal Cities

	(1) *BuyMore*	(2) *NetTrade*	(3) *NetRatio*	(4) *IvolTilt*	(5) *BetaTilt*	(6) *NonEpTilt*
ClimateVarHis× *VIX*	-0.0002	-0.0045**	-0.0010	-0.0006	-0.0003	-0.0092
	(0.0001)	(0.0021)	(0.0087)	(0.0004)	(0.0002)	(0.0141)
Controls	Y	Y	Y	Y	Y	Y
Client FE	Y	Y	Y	Y	Y	Y
Quarter FE	Y	Y	Y	Y	Y	Y
Observations	1,956,750	1,956,750	1,956,750	1,956,750	1,956,750	1,956,750
R-squared	0.267	0.438	0.109	0.166	0.145	0.155

Note: This table reports subsample analyses that probe the cultural-transmission interpretation of our baseline trading results (Tables 3 and 4). Panel A restricts the sample to investors whose birth prefecture has high *migration difficulty*—prefectures from which relocating to a climatically more stable region is costly—so that selective historical out-migration of more risk-tolerant individuals is unlikely to drive the result (the details are explained in section Appendix A5). The estimated effect remains negative and statistically significant, indicating the pattern is not an artifact of historical migration. Panel B restricts the sample to coastal prefectures, where the historical exchange of people and ideas was more frequent and cultural norms are therefore less sticky; consistent with cultural transmission, the effect is weaker and largely insignificant in these regions. Outcome variables, controls, fixed effects, and the sample period follow Table 3 and Table 4. *ClimateVarHis* is the standard deviation of prefecture-level PDSI (1500–1950) and *VIX* is the quarterly average of the daily SZ50 VIX index minus 10. All continuous variables are winsorized at the top and bottom 1% levels. Standard errors are clustered at the investor's hometown city level and are reported in parentheses. *** $p < 0.01$, ** $p < 0.05$, * $p < 0.10$.

C: Additional Analysis for Section V

Table C.1: Summary Statistics for Table 8 using CFPS

Var.	No.	Mean	Std	P10	Median	P90
Historical Climate Variability	19,061	1.422	0.404	0.985	1.334	2.036
Contemporary Climate Variability	19,061	2.104	0.430	1.599	2.090	2.680
EPU	19,061	1.853	0.989	0.921	1.062	3.634
Entrepreneur	19,061	0.111	0.314	0.000	0.000	1.000
Fin Lev	19,061	54.513	229.441	0.000	0.000	86.022
CashRatio	19,061	10.043	15.907	0.000	2.685	30.000
Total Asset	19,061	63.467	111.318	5.744	26.756	142.000
Housing Asset	19,061	45.639	89.809	1.000	17.500	100.000
Income	19,061	7.666	7.978	1.300	5.400	15.750
Expense	19,061	7.077	7.012	1.566	4.920	15.000
Family Size	19,061	3.049	1.305	2.000	3.000	5.000
Rural	19,061	0.779	0.415	0.000	1.000	1.000
House Loan	19,061	0.114	0.318	0.000	0.000	1.000
GDP Per Capita	19,061	0.052	0.037	0.018	0.040	0.102
GDP Ratio	19,061	7.342	6.949	-1.138	7.772	14.889

Notes: This table shows the summary statistics of variables in CFPS household tests. The sample is restricted to households whose registered residence has never changed across cities. *Entrepreneur* equals 1 if the household operates its own business. *Fin Lev* is non-financial debt divided by total assets, in %. *CashRatio* is cash holdings divided by total assets, in %. *Historical Climate Variability* is defined as the standard deviation of the PDSI for the household's city of residence from 1500 to 1950, while *Contemporary Climate Variability* is the standard deviation from 1950 to 2000. *EPU* denotes the yearly mean of the monthly Economic Policy Uncertainty index in the previous year, scaled by 100. Control variables include household total assets (in 10K RMB), expenditures (in 10K RMB), income (in 10K RMB), housing property (in 10K RMB), family size, a rural-resident dummy, and a house loan-holding dummy, as well as last-year local GDP per capita (in 1M RMB) and GDP growth rate. All continuous variables are winsorized at top and bottom 1% level.

Table C.2: Summary Statistics for Table 9 using CSMAR

Var.	No.	Mean	Std	P10	Median	P90
Historical Climate Variability	2,436	1.370	0.325	1.117	1.295	1.966
Contemporary Climate Variability	2,436	1.837	0.393	1.511	1.624	2.617
EPU	2,436	2.083	1.038	0.955	2.066	3.634
R&D Ratio	2,436	2.798	2.695	0.007	2.237	6.141
M&A	2,436	0.455	0.908	0.000	0.000	1.000
Ivol	2,436	0.025	0.008	0.016	0.024	0.035
Lev	2,436	0.389	0.201	0.132	0.385	0.660
Asset	2,436	111.605	307.537	8.981	32.226	178.773
CashRatio	2,436	0.175	0.143	0.041	0.130	0.373
BM	2,436	0.564	0.237	0.243	0.559	0.886
ROE	2,436	0.058	0.122	-0.019	0.064	0.172
Rtn	2,436	0.145	0.552	-0.387	0.013	0.848
Age	2,436	53.226	6.553	45.000	53.000	61.000
GDP Per Capita	2,436	0.083	0.037	0.041	0.075	0.129
GDP Ratio	2,436	0.093	0.047	0.037	0.089	0.156

Notes: This table reports the summary statistics for the variables used in the CEO-level analysis. *Historical Climate Variability* is defined as the standard deviation of the CEO's birth province's PDSI from 1500 to 1950, and *Contemporary Climate Variability* is the standard deviation from 1950 to 2000. *EPU* denotes the annual average of the monthly Economic Policy Uncertainty index, scaled by 100. The *R&D ratio* is measured as R&D expenditure divided by last year's total assets, in %. *M&A* represents the number of mergers and acquisitions in a given year. *Ivol* denotes idiosyncratic volatility (dropping stock–year observations with fewer than 60 daily returns). Other variables include total assets (in 100 million RMB), leverage, cash ratio, book-to-market ratio, ROE, annual stock return, CEO age, and the GDP per capita and GDP growth rate of the firm's province of location. All continuous variables are winsorized at the top and bottom 1% level.

Table C.3: Robustness: Alternative Measure for Climate Variability

Dep. Var.	(1)	(2)	(3)
	Entrepreneur (0/1)	Fin Debt / Asset	Cash / Asset
Extreme Weather Shocks × *EPU*	-0.0111**	-9.0308**	0.6954**
	(0.0048)	(4.2548)	(0.3341)
Household FE	Y	Y	Y
Year FE	Y	Y	Y
Household-level controls	Y	Y	Y
Birth-city controls	Y	Y	Y
Observations	19,061	19,061	19,061
R-squared	0.729	0.729	0.591

Note: This table replicates Table 8 in the main paper, replacing the primary climate-variability measure (SD of PDSI 1500–1950) with the total number of extreme weather events over 1500–1950 (years with |PDSI| > 2). All other variables and model specifications follow Table 8. All continuous variables are winsorized at the top and bottom 1% levels. Standard errors are clustered at the city level and reported in parentheses. *** $p < 0.01$, ** $p < 0.05$, * $p < 0.10$.

Acknowledgement

Yun Cong: No potential conflicts of interest

Pei Gao: No potential conflicts of interest

Yan Luo: No potential conflicts of interest

Yiqing Lv: No potential conflicts of interest